1969

A finite element method for geometrically nonlinear large displacement problems in thin, elastic plates and shells

Ronald August Melliere

A FINITE ELEMENT METHOD FOR GEOMETRICALLY NONLINEAR LARGE DISPLACEMENT PROBLEMS IN THIN, ELASTIC PLATES AND SHELLS

by

RONALD AUGUST MELLIERE, 1944-

A DISSERTATION

Presented to the Faculty of the Graduate School of the

UNIVERSITY OF MISSOURI - ROLLA

In Partial Fulfillment of the Requirements for the Degree

DOCTOR OF PHILOSOPHY

in

MECHANICAL ENGINEERING

1969

Harold Dean Keith
Advisor

Glen Wallace

J. R. Fawcett

Robert L. Davis

Clark R. Barker

Wm. S. Gatley

ABSTRACT

A finite element method is presented for geometrically nonlinear large displacement problems in thin, elastic plates and shells of arbitrary shape and boundary conditions subject to externally applied concentrated or distributed loading. The initially flat plate or curved shell is idealized as an assemblage of flat, triangular plate, finite elements representing both membrane and flexural properties. The 'geometrical' stiffness of the resulting eighteen degree-of-freedom triangular element is derived from a purely geometrical standpoint. This stiffness in conjunction with the standard small displacement 'elastic' stiffness is used in the linear-incremental approach to obtain numerical solutions to the large displacement problem. Only stable equilibrium configurations are considered and engineering strains are assumed to remain small. Four examples are presented to demonstrate the validity and versatility of the method and to point out its deficiencies.

PREFACE

In recent years, the theory of thin plates and shells (curved plates) has been one of the more active branches of the theory of elasticity. This is understandable in light of the fact that thin-walled shell constructions combine light weight with high strength, as a result of which they have found wide applications in naval, aeronautical and boiler engineering as well as in reinforced concrete roof designs. The practical possibilities for the utilization of thin plates and shells have by no means been exhausted. The engineer is continually made aware of the extension of the range of their employment and of the need for a more thorough analysis of their properties (i.e. an improvement of the methods of stress analysis).

The work presented herein is devoted to the analysis of nonlinear deformations and displacements in thin, elastic plates and shells. The nonlinearity of the problems treated in this dissertation is that associated with large displacements in the linear elastic range. In contrast to linear theory in which displacements must be small in comparison to the thickness of the plate or shell, the method presented is not restricted by the magnitude of the displacements provided that the engineering strains do not exceed the limit of proportionality and structural instability does not occur.

ACKNOWLEDGEMENTS

The author wishes to express his sincere appreciation to Dr. H. D. Keith for his extreme patience and unselfish guidance and assistance throughout the course of this work.

In addition, the author would like to thank Dr. T. R. Faucett, Dr. W. S. Gatley, Dr. C. R. Barker, Dr. R. L. Davis, and Dr. G. Haddock for serving as members of his thesis committee. In particular, the timely suggestions and encouragement of Dr. R. L. Davis are gratefully acknowledged.

TABLE OF CONTENTS

Chapter Page

LIST OF ILLUSTRATIONS

NOMENCLATURE AND LIST OF SYMBOLS

The following symbols are used in this presentation. A tilde ($\sim$) indicates the quantity is a function of spatial coordinates. A prime (') denotes a quantity associated with the local coordinate system.

*, **	- footnote symbols,
$[\ ]$	- matrix of dimensions r X s,
$\{\ \}$	- column matrix (vector) of dimensions r X 1,
$[\ ]^T$	- transpose of a matrix,
$[\ ]^{-1}$	- inverse of a square matrix,
x, y, z; x', y', z'	- global and local coordinates,
u, v, w, θ_x, θ_y, θ_z	- generalized global displacements,
u', v', w', θ_x', θ_y', θ_z'	- generalized local displacements,
F_x, F_y, F_z, M_x, M_y, M_z	- generalized global forces,
F_x', F_y', F_z', M_x', M_y', M_z'	- generalized local forces,
i, j, k	- nodes of the triangular element,
$\{\delta_i\}$	- global nodal displacement vector,
b, p	- superscripts denoting bending and in-plane action quantities,
$\{\delta_i^{b'}\}$, $\{\delta_i^{p'}\}$, $\{\delta_i'\}$	- local nodal displacement vectors for bending, in-plane, and combined actions,
$\{F_i\}$	- global nodal force vector,
$\{F_i^{b'}\}$, $\{F_i^{p'}\}$, $\{F_i'\}$	- local nodal force vectors for bending, in-plane, and combined actions,
u_o, v_o, w_o	- displacements of the middle surface,
ϵ_x, ϵ_y, γ_{xy}	- engineering strains,
σ_x, σ_y, τ_{xy}	- engineering stresses,

E - modulus of elasticity,

E, G - subscripts denoting elastic and geometric quantities,

υ - Poisson's ratio,

N_x, N_y, N_{xy} - stress resultants in plate theory,

M_x, M_y, M_{xy} - stress couples (moments) in plate theory,

q - distributed loading,

h - plate thickness,

∇^2 - harmonic operator,

∇^4 - biharmonic operator,

n - subscript indicating incremental step number,

Δ - denotes an incremental change,

$\{R\}$ - external nodal load vector for the assembled structure,

$\{\delta\}$ - nodal displacement vector for the assembled structure,

e - superscript denoting a quantity associated with a particular element,

$\{F\}^e$, $\{F'\}^e$ - element global and local nodal force vectors,

$\{\delta\}^e$, $\{\delta'\}^e$ - element global and local nodal displacement vectors,

$[k]^e$ - element global incremental stiffness matrix,

$[k']^e$, $[k_{rs}']^e$ - element local elastic stiffness matrix and submatrices,

$[T]^e$ - element transformation matrix of direction cosines,

$\{F_E\}^e$, $\{F_G\}^e$ - element global nodal force vectors for elastic and geometric actions,

$[k_E]^e$, $[k_G]^e$ - element global stiffness matrices for elastic and geometric actions,

$[k]$ - global stiffness matrix for assembled structure,

a_1, a_2, c - triangular element dimensions,

m - superscript denoting triangular element subregion,

$\{\alpha\}$ - vector of constants for bending displacement expansions,

$t^{(m)}$, $r^{(m)}$ - constants in bending displacement expansions,

$\{\delta^{b'}\}$ - element local bending displacement vector,

$[C1]$ - matrix of local coordinate parameters,

$[\tilde{P}]^{(m)}$ - interpolation matrices for bending displacements,

$\{\tilde{K}^{b'}\}$ - generalized bending strain (curvature) vector,

$\tilde{K}_{x'}^{b}$, $\tilde{K}_{y'}^{b}$, $\tilde{K}_{x'y'}^{b}$ - generalized bending strains,

$\tilde{\epsilon}_{x'}^{b}$, $\tilde{\epsilon}_{y'}^{b}$, $\tilde{\gamma}_{x'y'}^{b}$ - bending engineering strains,

$\tilde{M}_{x'}^{b}$, $\tilde{M}_{y'}^{b}$, $\tilde{M}_{x'y'}^{b}$ - generalized bending stresses,

$\tilde{\sigma}_{x'}^{b}$, $\tilde{\sigma}_{y'}^{b}$, $\tilde{\tau}_{x'y'}^{b}$ - bending engineering stresses,

$\{\tilde{\sigma}^{b'}\}$ - bending engineering stress vector,

$\{\tilde{M}^{b'}\}$ - generalized bending stress vector,

$[\tilde{Q}]^{(m)}$, $[\tilde{B}^{b}]^{(m)}$ - bending strain interpolation matrices,

$[D^{b}]$ - bending elasticity matrix,

$[k^{b'}]$, $[k_{rs}{}^{b'}]$ - element bending stiffness matrix and submatrices,

V, A - element volume and mid-surface area,

$\{\beta\}$, $[CP]$ - matrices of constants for in-plane displacement expansions,

$\{\delta^{p'}\}$ - element in-plane displacement vector,

$\{\epsilon^{p'}\}$ - in-plane generalized strain vector,

$\tilde{\epsilon}_{x'^p}$, $\tilde{\epsilon}_{y'^p}$, $\tilde{\gamma}_{x'y'^p}$ - in-plane engineering strains,

$\left[B^p\right]$, $\left[B_i{}^p\right]$ - in-plane strain interpolation matrices,

$\left\{\tilde{\sigma}^{p'}\right\}$ - in-plane engineering stress vector,

$\tilde{\sigma}_{x'^p}$, $\tilde{\sigma}_{y'^p}$, $\tilde{\tau}_{x'y'^p}$ - in-plane engineering stresses,

$\left[D^p\right]$ - in-plane elasticity matrix,

$\left[k^{p'}\right]$, $\left[k_{rs}{}^{p'}\right]$ - element in-plane stiffness matrix and submatrices,

$\left[L\right]$, $\left[\lambda\right]$ - element transformation matrices of direction cosines,

$\left[F_{ii'}\right]$ - matrix of local nodal forces,

$\left[\partial / \partial \delta_i\right]$ - matrix of partial derivative operators,

$\left[k_{rs_E}\right]^e$, $\left[k_{rs_G}\right]^e$, $\left[k_{rs}\right]^e$ - element elastic, geometric, and incremental stiffness submatrices,

$\lambda_{r's}$ - direction cosines,

l_{ij}, l_{jk}, l_{ki} - length of triangular sides,

$\hat{e}_{x'}$, $\hat{e}_{y'}$, $\hat{e}_{z'}$ - unit vectors in x', y', and z' directions.

CHAPTER I

INTRODUCTION

The search for minimum-weight, optimum structural design has tended to cast doubt on the validity of the assumptions leading to linear formulation of the structural analysis problem. This in turn has generated considerable interest in the nonlinear analysis of structures. For example, in some cases it has become necessary to use more exact strain-displacement relations, to base the equilibrium conditions on the deformed configuration, and even to consider nonlinear material properties.

For the flexible, minimum-weight structures utilized in aerospace applications (e.g. thin plates and shells), a significant portion of practical design problems involve geometrically nonlinear behavior with linear, elastic material response. This relevance to realistic design situations has motivated the extension of the powerful finite element technique to account for geometric nonlinearities.

The objective of the work reported in this dissertation was to develop a finite element representation capable of predicting the geometrically nonlinear, large displacement behavior of thin, elastic plates and shells, and to demonstrate its validity. Plates and shells of arbitrary shape and boundary conditions subject to externally applied concentrated or distributed loading were considered.

CHAPTER II

PREVIOUS WORK

The finite element displacement method of structural analysis for linear structural systems is well established. Previous extensions of the method to treat the nonlinearities which may arise in the structural system due to large displacements may be divided into two major areas according to the extent of nonlinearity treated. The first area includes those approaches which treat the geometric nonlinearities caused by large displacements (1-12).* The second area includes those approaches which account for material as well as geometric nonlinearities (13-14).

The first area, the one of interest herein, can be further separated into three categories. The first includes those approaches that take geometric nonlinearity into account by solving a sequence of linear problems. These procedures are characterized by an incremental application of the loading, the use of stiffness matrices which include the influence of initial forces, and an updating of the nodal coordinates (1-5). The second category is composed of those techniques which account for geometric nonlinearity by formulating the set of nonlinear simultaneous equations governing the behavior of the structural system and then proceeding to a solution by successive approximations (9-10). Finally, the third category consists of those approaches that employ nonlinear strain-displacement relations to construct the potential

---

*Numbers underlined in parentheses refer to listings in Bibliography.

energy for each of the elements and hence for the entire structure, and then obtaining a numerical solution by seeking the minimum of the total potential energy (11-12).

In reference to geometrically nonlinear large displacement problems in thin plates and shells, a number of contributions have been made in recent years. Martin (2) derived an 'initial stress' stiffness matrix for the thin triangular element in plane stress. This stiffness matrix, for use in the linear-incremental approach, was derived by formulating the total strain energy in terms of nodal displacements and applying Castigliano's first theorem. In the formulation, nonlinear strain-displacement relations were used, the nonlinearity being associated with the second degree rotation terms normally neglected in small displacement theory. As a closing comment, Martin suggested that for large deflection problems in thin plates and shells the behavior of the thin triangular element in bending could be satisfactorily described by using the 'initial stress' stiffness matrix for the triangle in plane stress plus a conventional 'elastic' stiffness which has been found to be suitable for the case of small deflections. Unfortunately, at that time no data from such calculations was available and to this author's knowledge, none has been published to this date.

Argyris (4) derived the so-called 'geometrical' stiffness of the triangular element in plane stress for use in the linear-incremental approach to large displacement problems. The stiffness was formulated in terms of his 'natural' nodal force and displacement vectors. The derivation was made from a purely geometrical standpoint in which the 'geometrical' stiffness accounted for the change in nodal forces

arising in an incremental step due to the fact that the direction of the original forces, previously in equilibrium, had been altered. Argyris gave no examples of application of this approach to large displacement thin plate and shell problems but indicated that work in this area was forthcoming.

Murray and Wilson (6) solved the large deflection thin plate problem using triangular flat plate elements. The standard small displacement stiffness matrix was used in conjunction with an iterative procedure based on achieving an equilibrium balance. The precedure is equally applicable to large displacement shell problems since the initially flat plate becomes essentially a curved shell when the deflections become larger than the thickness. Comparison with known plate solutions was remarkably good.

Stricklin, et al. (8) applied the matrix displacement method to the nonlinear elastic analysis of shells of revolution subjected to arbitrary loading. The method employed linearized the nonlinear equilibrium equations by separating the linear and nonlinear portions of the strain energy and then applying the nonlinear terms as additional generalized forces. The resulting equilibrium equations were solved by one of three methods: The load-increment method, iteration, or a combination of the two. The nonlinear terms, being functions of the generalized displacements, were evaluated based on values of the coordinates at the previous load increment or values obtained during the previous iteration. Good agreement with experimental results was indicated.

Alzheimer and Davis (10) applied the method of successive

approximations to the nonlinear unsymmetrical bending of a thin annular plate. The nonlinear von Karman thin-plate equations were solved with an iteration technique utilizing the solution from linear theory as the first approximation. The results compared favorably to experimental data.

Schmit, et al. (12) employed nonlinear strain-displacement relations in constructing the potential energy for large deflections of rectangular plate and cylindrical shell discrete elements. The total potential energy for the entire structure was formulated with the inclusion of geometric nonlinearities in the strain-displacement relations. An approximate solution was obtained numerically by direct minimization of this total potential energy. The principal limitation on the method is that the rotations of the deformed configuration relative to the undeformed structure must be small.

Nowhere in the literature does there seem to be an implementation and verification of a method for geometrically nonlinear large displacement problems in arbitrary thin, elastic plates and shells. In particular, the linear-incremental approach characterized by the so-called 'geometrical' stiffness suggested by Zienkiewicz (15) and originated by Argyris (5), does not seem to have been utilized in the analysis of large displacement problems in thin plates and shells. This concept is the one utilized and demonstrated in this dissertation.

CHAPTER III

REVIEW OF FINITE ELEMENT CONCEPTS

In the finite element method, the behavior of an actual structure is simulated by approximating it with that of a model consisting of subregions or 'elements' interconnected at nodal points. In each element the displacement field is restricted to a linear combination of pre-selected displacement patterns or 'shape functions.' Thus the configuration of the model is determined by the magnitudes of the generalized coordinates associated with the shape functions. The displacement state which minimizes the total potential energy is determined and this configuration is then interpreted as an approximation to the true configuration of the structure under a set of applied loads. How accurately the model represents the true behavior of the structure depends to a large extent on the displacement patterns selected and the compatibility conditions imposed along element boundaries.

In an effort to ensure that the behavior of the model is a close approximation to the true displacement state, certain minimum requirements of displacement functions should be adhered to. They are given by Zienkiewicz (15) on page 22 as follows:

(i) Completeness Requirements: The displacement functions chosen should permit rigid body displacements (zero strain) and include the constant-strain states associated with the problem of interest.

(ii) Compatibility Requirements: The displacement state produced should provide continuity of displacements throughout the

interior of the element and along the boundary with adjacent elements.

The solution of the problem requires first the evaluation of the stiffness properties of the individual elements. The stiffness properties of the entire structure are then obtained by superposition of the element stiffnesses. Finally, analysis of the structure is accomplished by solution of the simultaneous nodal point equilibrium equations for the nodal displacements.

CHAPTER IV

SHELL THEORY

A. STRUCTURAL IDEALIZATION

A curved-shell structure is in essence a singly (or doubly) curved thin plate. The detailed derivation of the governing equations for curved-shell problems presents many difficulties which lead to alternate formulations depending upon the assumptions made. Various numerical procedures have been formulated to deal with special geometric shapes but these are severely limited in applicability. In the finite element representation of shell structures these difficulties are eliminated by assuming that the behavior of a continuously-curved surface can be adequately approximated by that of a surface built up of small, flat plate elements.

In the work presented herein, the curved shell structure of arbitrary geometry is modeled as a surface built up of triangular flat plate elements, the corner (or nodal) points of which lie on the mid-surface of the actual shell as shown in Figure 1(a). These elements are capable of adequately representing the arbitrary geometry considered and are assumed to exhibit the bending and in-plane behavior that the actual shell experiences. Any externally applied concentrated or distributed loading is considered, no limitations are imposed with regard to boundary conditions, and the shell properties may vary in any specific fashion from one point on the middle surface to another. As suggested by Zienkiewicz (15) on page 125, in accordance with the physical effect of replacing a curved surface with a collection of plane elements, any

distributed loading will be concentrated as statically equivalent nodal forces.

It should be pointed out that the foregoing idealization of the shell introduces two forms of approximations. First, the collection of flat-plate elements provides only an approximation to the smoothly curved surface of the actual shell. Second, the stiffness properties of the individual elements are based upon assumed displacement patterns within the elements, imposing constraints on the manner of deformations of the shell. However, these imposed errors should diminish as the mesh size is reduced.

As illustrated in Figure 1, two distinct right-handed cartesian coordinate systems will be considered. First, a 'global' coordinate system x-y-z, common to all elements, is defined. This coordinate system will be used for assembly of the overall structural properties. Second, a separate 'local' coordinate system* x'-y'-z' is defined for each element. The element properties will be evaluated first in the local coordinate systems and then transformed to global orientation for assembly.

For the general three-dimensional shell problem six degrees of freedom per node will be considered. These are given by displacement components u, v, and w in the x, y, and z directions and rotations θ_x, θ_y, and θ_z (directed according to the right-hand rule) about the x, y, and z axes, respectively. The corresponding generalized forces include the force components F_x, F_y, and F_z in the x, y, and z directions

---

*Quantities referred to the local coordinate directions are denoted by primes to distinguish them from those associated with global coordinates.

and the moments M_x, M_y, and M_z about the x, y, and z axes, respectively. In matrix notation* the resulting 'global' displacement and force vectors for node 'i' are, respectively

$$\{\delta_i\} = \begin{Bmatrix} u_i \\ v_i \\ w_i \\ \theta_{x_i} \\ \theta_{y_i} \\ \theta_{z_i} \end{Bmatrix} \qquad \text{(A-1)}^{**}$$

and

$$\{F_i\} = \begin{Bmatrix} F_{x_i} \\ F_{y_i} \\ F_{z_i} \\ M_{x_i} \\ M_{y_i} \\ M_{z_i} \end{Bmatrix} . \qquad \text{(A-2)}$$

The corresponding vectors for node 'i' in 'local' coordinates are, respectively

---

*Matrix notation will be employed throughout this dissertation with symbolic representations defined on page x.

**Numbers in parentheses refer to equations.

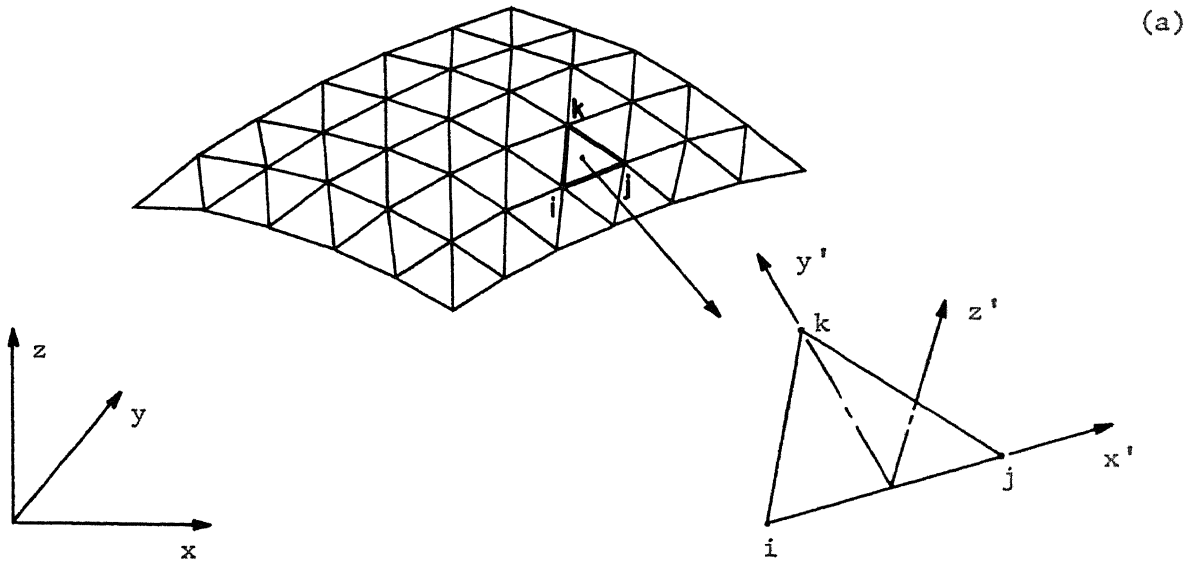

Global Frame

Local Frame

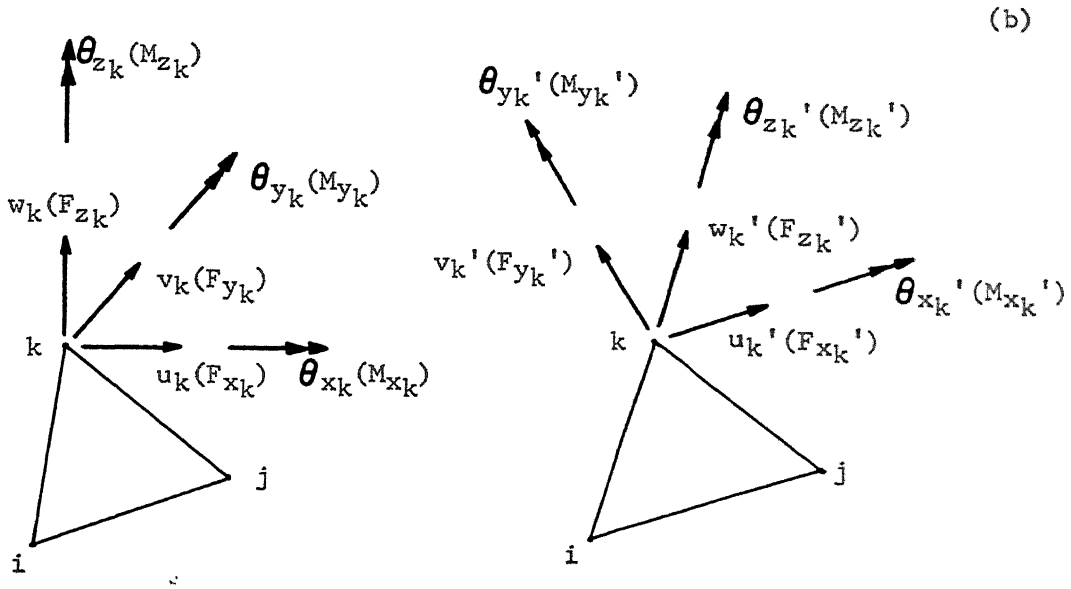

Global Components

Local Components

Figure 1. A Typical Finite Element Idealization of a Shell Structure.

$$\{\delta_i'\} = \begin{Bmatrix} u_i' \\ v_i' \\ w_i' \\ \theta_{x_i}' \\ \theta_{y_i}' \\ \theta_{z_i}' \end{Bmatrix} \tag{A-3}$$

and

$$\{F_i'\} = \begin{Bmatrix} F_{x_i}' \\ F_{y_i}' \\ F_{z_i}' \\ M_{x_i}' \\ M_{y_i}' \\ M_{z_i}' \end{Bmatrix} . \tag{A-4}$$

These generalized displacements and forces in global and local coordinates are illustrated in Figure 1(b) for a typical node 'k' of a typical triangular element i-j-k.

B. LARGE DISPLACEMENT FINITE ELEMENT ANALYSIS

1. GENERAL LARGE DISPLACEMENT THEORY

The general large displacement problem in finite element analysis may differ from the small displacement problem in the following respects:

Due to large displacements --

(i) Geometric nonlinearities may arise as a result of

i.1. product terms in the strain-displacement relation, and/or

i.2. the effect of deformation on the equilibrium equations, and/or

i.3. the effect of deformation on the size and shape of the elements.

(ii) Material nonlinearities may arise in the individual elements due to the occurrence of large strains.

2. LARGE DISPLACEMENT SHELL THEORY

The large displacement problems treated in this dissertation are those in which the strains within the material are small and the material behaves in a linear-elastic manner. That is, all strains are assumed to be within the elastic limit. In addition, only well-defined, unique, and stable equilibrium configurations will be considered. Thus the buckling problem will not be treated, although post-buckling behavior is within the scope of the method presented.

In accordance with the chosen finite element idealization and the above restrictions, the large displacement problem in thin, elastic shells (and plates) has been reduced to the geometrically nonlinear large displacement analysis of a thin, triangular, flat-plate element. The geometrical nonlinearity of the problem will be shown to be due primarily to the rigid body rotations associated with the out-of-plane displacement component, w'.

(a) THIN-PLATE THEORY

A thin plate is one in which the ratio of plate thickness to a characteristic lateral dimension is small. In the large deflection thin-plate problem the engineering strains, but not the rotations, can be considered as infinitesimal. The physical consideration which differentiates between small and large deflection plate theories is the

stretching of the middle surface as a result of out-of-plane bending deformation. In small deflection theory the resulting 'membrane' stresses are not accounted for. Small deflection theory can be considered applicable "only if the stresses corresponding to this stretching of the middle surface are small in comparison with the maximum bending stresses." This will be true "if the deflections of a plate from its initial plane or from a true developable surface are small in comparison with the thickness of the plate."*

Accepting the first quotation above as the distinguishing feature separating 'large' from 'small' deflection plate theories, the limit of applicability of small deflection theory cannot be associated with any absolute geometric restriction on displacements or rotations. However, the limit generally accepted is that the ratio of maximum deflection to plate thickness must be less than $\frac{1}{2}$, although this can be influenced by factors such as boundary conditions.

Since finite element solutions will, for some problems, be compared to solutions from classical plate theory it will be helpful to list below the equations from classical theory for small and large displacements and to point out the assumptions made in their derivation.

Restrictions on the Displacement Field.

For thin plates the following restrictions can be placed on the displacement field:

(i) Material points lying on normals to the middle surface before deformation remain in a straight line after deformation

---

*Quotations are from pages 48 and 49 of Timoshenko (17).

(normals remain straight).

(ii) The straight line through the material points referred to in (i) is also normal to the middle surface after deformation (normals remain normal).

(iii) The strain in the direction of the normal can be neglected in establishing the displacement of a material point.

(iv) The slope of the middle surface remains small with respect to the initial plane.

Assumptions (i), (ii), and (iii) are usually referred to as the 'Kirchoff Assumptions.' In addition to the above, the following restrictions on displacement gradients also apply:*

$$\text{(v)}\quad u_{,x},^{**}\ u_{,y},\ v_{,x},\ v_{,y},\ w_{,z} << 1 \tag{B-1}$$

are required to be small quantities of second order and

$$\text{(vi)}\quad w_{,x},\ w_{,y} < 1 \tag{B-2}$$

are required to be small quantities of first order such that the square of these quantities, which is of second order, is of the same order as the engineering strains and the quantities in (v).

---

*In this section the coordinate x-y plane is the middle surface of the flat plate before deformation. In finite element theory this would be the local coordinate x'-y' plane.

**The comma (,) denotes a partial derivative with respect to the variable subscript; e.g. $u_{,x} = \frac{\partial u}{\partial x}$.

Derivation of the Thin-Plate Equations

The above restrictions on the displacement field are applied in deriving the following relations:

(i) The Kirchoff Equations;

$$\begin{aligned} u(x,y,z) &= u_o(x,y) - z\, w_o(x,y),x \\ v(x,y,z) &= v_o(x,y) - z\, w_o(x,y),y \\ w(x,y,z) &= w_o(x,y) \end{aligned} \tag{B-3}$$

where u_o, v_o, and w_o are the displacements of the middle surface in the x, y, and z directions, respectively.

(ii) The engineering strain-displacement relations;

$$\begin{aligned} \epsilon_x &= u,x + \tfrac{1}{2}(w,x)^2 \\ \epsilon_y &= v,y + \tfrac{1}{2}(w,y)^2 \\ \gamma_{xy} &= u,y + v,x + w,x\, w,y \ . \end{aligned} \tag{B-4}$$

(iii) The stress-strain relations (homogeneous, isotropic, elastic material);

$$\begin{Bmatrix} \sigma_x \\ \sigma_y \\ \tau_{xy} \end{Bmatrix} = \frac{E}{1-\nu^2} \begin{bmatrix} 1 & \nu & 0 \\ \nu & 1 & 0 \\ 0 & 0 & \frac{1-\nu}{2} \end{bmatrix} \begin{Bmatrix} \epsilon_x \\ \epsilon_y \\ \gamma_{xy} \end{Bmatrix} \tag{B-5}$$

where E is Young's modulus and ν, Poisson's ratio.

(iv) The equilibrium equations;

$$
\begin{aligned}
&N_{x,x} + N_{yx,y} = 0 \\
&N_{xy,x} + N_{y,y} = 0 \\
&M_{x,xx} + 2M_{xy,xy} + M_{y,yy} = \\
&\qquad -\left[q + N_x w_{o,xx} + 2 N_{xy} w_{o,xy} + N_y w_{o,yy} \right]
\end{aligned}
\tag{B-6}
$$

where N_x, N_y, and N_{xy} are stress resultants, M_x, M_y, and M_{xy} are stress couples and q is the distributed loading. The stress resultants and couples are illustrated in Figure 2 and defined respectively as

$$
\begin{Bmatrix} N_x \\ N_y \\ N_{xy} \end{Bmatrix} = \int_{-\frac{h}{2}}^{\frac{h}{2}} \begin{Bmatrix} \sigma_x \\ \sigma_y \\ \tau_{xy} \end{Bmatrix} dz \tag{B-7}
$$

and

$$
\begin{Bmatrix} M_x \\ M_y \\ M_{xy} \end{Bmatrix} = \int_{-\frac{h}{2}}^{\frac{h}{2}} \begin{Bmatrix} \sigma_x \\ \sigma_y \\ \tau_{xy} \end{Bmatrix} z\, dz \tag{B-8}
$$

for a plate of thickness h.

(b) SMALL DEFLECTION PLATE EQUATIONS

The small deflection equations may be obtained by imposing restrictions (B-1) on all displacement gradients. The product terms in (B-4) may then be omitted since they are small quantities of higher order. The stress resultants and stress couples then become

(a)

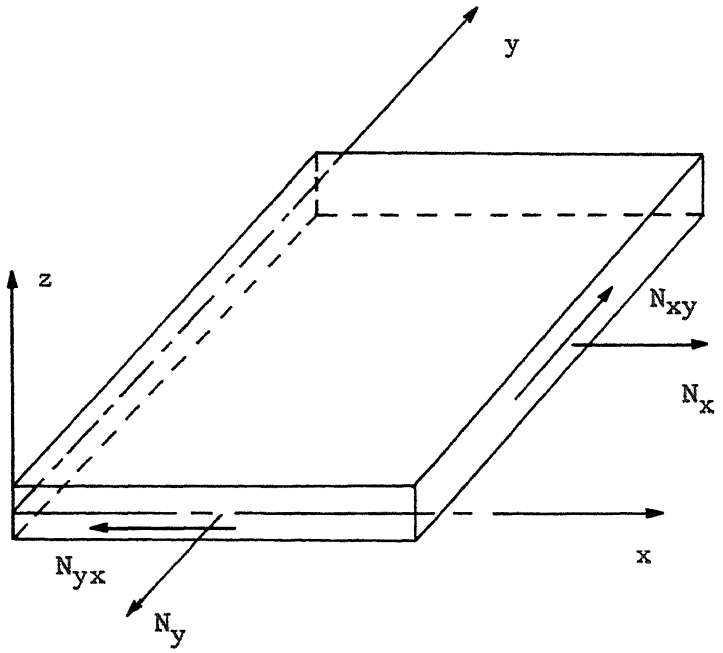

Stress Resultants

(b)

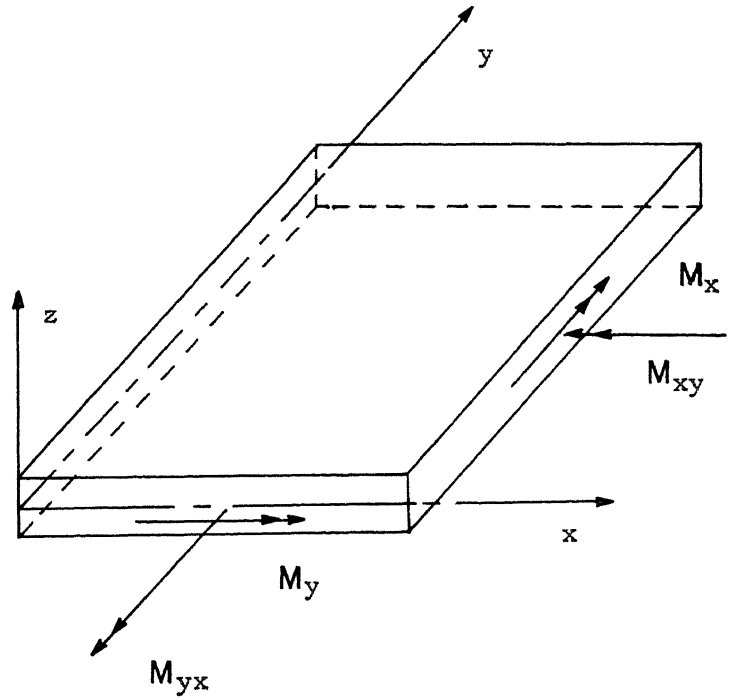

Stress Couples

Figure 2. Stress Resultants and Stress Couples in Plate Theory.

$$\begin{Bmatrix} N_x \\ N_y \\ N_{xy} \end{Bmatrix} = \frac{Eh}{1-\nu^2} \begin{bmatrix} 1 & 0 & 0 & \nu \\ \nu & 0 & 0 & 1 \\ 0 & \frac{1-\nu}{2} & \frac{1-\nu}{2} & 0 \end{bmatrix} \begin{Bmatrix} u_o,x \\ u_o,y \\ v_o,x \\ v_o,y \end{Bmatrix} \tag{B-9}$$

$$\begin{Bmatrix} M_x \\ M_y \\ M_{xy} \end{Bmatrix} = \frac{-Eh^3}{12(1-\nu^2)} \begin{bmatrix} 1 & \nu & 0 \\ \nu & 1 & 0 \\ 0 & 0 & \frac{1-\nu}{2} \end{bmatrix} \begin{Bmatrix} w_o,xx \\ w_o,yy \\ 2\, w_o,xy \end{Bmatrix} . \tag{B-10}$$

The displacement equations of equilibrium become

$$\begin{aligned} \nabla^2 u_o - \left(\frac{1+\nu}{2}\right)(u_o,yy - v_o,xy) &= 0 \\ \nabla^2 v_o - \left(\frac{1+\nu}{2}\right)(v_o,xx - u_o,xy) &= 0 \\ \nabla^4 w_o = \frac{12(1-\nu^2)}{Eh^3}(q + N_x w_o,xx + 2 N_{xy} w_o,xy + N_y w_o,yy) \end{aligned} \tag{B-11}$$

where ∇^2 is the harmonic operator $\left(\frac{\partial^2}{\partial x^2} + \frac{\partial^2}{\partial y^2}\right)$ and ∇^4 is the biharmonic operator $\left(\frac{\partial^4}{\partial x^4} + 2\frac{\partial^4}{\partial x^2 \partial y^2} + \frac{\partial^4}{\partial y^4}\right)$.

The first two of Equations (B-11) represent the displacement equations of equilibrium of the plane stress problem and are coupled together. They are, however, uncoupled from the third equation which represents the equilibrium equation for out-of-plane displacement. Thus for small deflections, the in-plane and out-of-plane behavior of thin plates are independent although the in-plane equations must be solved first.

(c) LARGE DEFLECTION PLATE EQUATIONS

The nonlinear von Karman equations for large deflection of thin plates are obtained by retaining the product terms in Equation (B-4) and proceeding in the same manner as for the small deflection theory.* The stress resultants and stress couples then become

$$N_x = \frac{Eh}{1-\nu^2}\left(u_{o,x} + \frac{(w_{o,x})^2}{2} + \nu\left(v_{o,y} + \frac{(w_{o,y})^2}{2}\right)\right)$$

$$N_y = \frac{Eh}{1-\nu^2}\left(v_{o,y} + \frac{(w_{o,y})^2}{2} + \nu\left(u_{o,x} + \frac{(w_{o,x})^2}{2}\right)\right) \qquad \text{(B-12)}$$

$$N_{xy} = \frac{Eh}{2(1+\nu)}\left(u_{o,y} + v_{o,x} + w_{o,x}\, w_{o,y}\right)$$

and

$$\begin{Bmatrix} M_x \\ M_y \\ M_{xy} \end{Bmatrix} = \frac{-Eh^3}{12(1-\nu^2)} \begin{bmatrix} 1 & \nu & 0 \\ \nu & 1 & 0 \\ 0 & 0 & \frac{1-\nu}{2} \end{bmatrix} \begin{Bmatrix} w_{o,xx} \\ w_{o,yy} \\ 2w_{o,xy} \end{Bmatrix} . \qquad \text{(B-13)}$$

The displacement equations of equilibrium are given by

$$\frac{\partial}{\partial x}\left(u_{o,x} + \nu\, v_{o,y} + \tfrac{1}{2}\left((w_{o,x})^2 + \nu\,(w_{o,y})^2\right)\right) + \frac{1-\nu}{2}\frac{\partial}{\partial y}\left(u_{o,y} + v_{o,x} + w_{o,x}\, w_{o,y}\right) = 0$$

$$\frac{\partial}{\partial y}\left(v_{o,y} + \nu\, u_{o,x} + \tfrac{1}{2}\left((w_{o,y})^2 + \nu\,(w_{o,x})^2\right)\right) + \frac{1-\nu}{2}\frac{\partial}{\partial x}\left(u_{o,y} + v_{o,x} + w_{o,x}\, w_{o,y}\right) = 0 \qquad \text{(B-14)}$$

$$\nabla^4 w_o = \frac{12(1-\nu^2)}{Eh^3}\left(q + N_x\, w_{o,xx} + 2N_{xy}\, w_{o,xy} + N_y\, w_{o,yy}\right) .$$

---

*The detailed derivation of the small and large deflection plate equations is not of interest here and has not been included. The details can be found in the standard texts on plate theory.

Now, however, the first two of Equations (B-14), which represent the in-plane behavior, are dependent on w_o. The third equation representing the out-of-plane equilibrium is dependent on the in-plane displacements u_o and v_o due to the presence of the stress resultants N_x, N_y, and N_{xy} (see Equation (B-12)). Thus the in-plane and out-of-plane behavior are completely coupled for large displacements.

It is significant to note that the only difference between the small and large displacement formulations is the inclusion of the product terms in the strain-displacement relations (B-4). These terms are physically the rotation terms associated with the out-of-plane displacement component, w.

In the development of the finite element method which follows, restrictions (B-1) are placed on all displacement gradients with respect to 'local' coordinates for the displacement increments obtained in each linear-incremental step. However, since the local coordinate system translates and rotates with the element, all of the above restrictions on displacement gradients can be removed with respect to global coordinates for the total displacements from the initial configuration.

3. THE LINEAR-INCREMENTAL APPROACH

In the linear-incremental finite element approach to the 'geometrically' nonlinear large displacement problem, the loading is divided into a number of equal or varied steps whose size is chosen to yield displacement increments sufficiently small such that linear theory applies. To the entire structure which is in equilibrium at the conclusion of step (n), an incremental external load vector $\Delta\{R\}_{n+1}$

is applied to yield the incremental displacements $\Delta\{\delta\}_{n+1}$. These incremental displacements, which determine the incremental strains and stresses, are added to the previous nodal locations to establish the updated position vector defining the structural configuration at the end of step (n+1). This process is repeated until the entire load has been applied. For each step linear theory is applied in the form of a linear relationship between incremental loads and displacements. The stiffness matrix expressing this linear relation must, however, include the 'geometrical' effect of large displacements as well as the 'elastic' effect encountered during small displacements.

For element 'e' the incremental stiffness called for above can be determined by considering the element in equilibrium before and after the (n+1)st step. For the assumed conditions of small engineering strains and linear steps, the elemental 'elastic' stiffness suitable for small displacements clearly remains the same throughout the step relative to the local coordinate system attached to and moving with the element. This stiffness is denoted by $[k']^e$.* The element undergoes a change of displacement $\Delta\{\delta\}^e_{n+1}$ during step (n+1). The element 'incremental' stiffness relates the incremental change in nodal forces to these incremental displacements. This stiffness is the one desired and is defined by the relation

$$\Delta\{F\}^e_{n+1} = [k]^e_{n+1}\ \Delta\{\delta\}^e_{n+1} \quad . \tag{B-15}$$

---

*The superscript 'e' denotes those quantities associated with a particular element (e) to distinguish them from quantities associated with the assembled structure.

The elemental forces and displacements in local coordinates are related to the corresponding global quantities by the standard transformation matrix of direction cosines $\left[T\right]^e$ between the two coordinate systems. This relationship is expressed by

$$\begin{aligned} \left\{F'\right\}^e &= \left[T\right]^e \left\{F\right\}^e \\ \left\{\delta'\right\}^e &= \left[T\right]^e \left\{\delta\right\}^e \quad . \end{aligned} \tag{B-16}$$

At the conclusion of step (n) the element was in equilibrium under the local nodal forces $\left\{F_n'\right\}^e$ whose global components are identified as

$$\left\{F_n\right\}^e = \left[T_n\right]^{Te} \left\{F_n'\right\}^e \tag{B-17}$$

by noting that the transformation matrix is orthogonal.

During step (n+1) the transformation matrix $\left[T_n\right]^e$ undergoes a change $\left[\Delta T_{n+1}\right]^e$ since it is a function of nodal coordinates and hence displacements. In addition, the local nodal forces $\left\{F_n'\right\}^e$ undergo a change $\Delta\left\{F'\right\}^e_{n+1}$ due to straining of the element. Thus, at the conclusion of step (n+1) the element is in equilibrium under the nodal loads

$$\begin{aligned} \left\{F_{n+1}\right\}^e &= \left[T_n + \Delta T_{n+1}\right]^{Te} \left\{F_n' + \Delta F_{n+1}'\right\}^e \\ &= \left[T_n\right]^{Te} \left\{F_n'\right\}^e + \left[T_n + \Delta T_{n+1}\right]^{Te} \Delta\left\{F'\right\}^e_{n+1} \\ &\quad + \left[\Delta T_{n+1}\right]^{Te} \left\{F_n'\right\}^e \end{aligned} \tag{B-18}$$

in which the incremental nodal forces due to local straining are given by

$$\Delta\left\{F'\right\}^{e}_{n+1} = \left[k'\right]^{e} \Delta\left\{\delta'\right\}^{e}_{n+1} \quad . \tag{B-19}$$

Applying the second of Equations (B-16), this becomes

$$\Delta\left\{F'\right\}^{e}_{n+1} = \left[k'\right]^{e} \left[T_n + \Delta T_{n+1}\right]^{e} \Delta\left\{\delta\right\}^{e}_{n+1} \quad . \tag{B-20}$$

By employing Equations (B-20) and (B-17), Equation (B-18) can be written as

$$\Delta\left\{F\right\}^{e}_{n+1} = \Delta\left\{F_E\right\}^{e}_{n+1} + \Delta\left\{F_G\right\}^{e}_{n+1} \tag{B-21}$$

if the incremental nodal forces are defined as

$$\Delta\left\{F\right\}^{e}_{n+1} = \left\{F_{n+1}\right\}^{e} - \left\{F_n\right\}^{e} \tag{B-22}$$

and the two terms on the right in Equation (B-21) are defined as follows. The first term represents the incremental nodal forces due to 'Elastic' straining of the element and is expressed by

$$\Delta\left\{F_E\right\}^{e}_{n+1} = \left[T_n + \Delta T_{n+1}\right]^{T\,e} \left[k'\right]^{e} \left[T_n + \Delta T_{n+1}\right]^{e} \cdot \Delta\left\{\delta\right\}^{e}_{n+1} \quad . \tag{B-23}$$

For sufficiently small steps $\left[\Delta T_{n+1}\right]^{e}$ can be neglected in comparison to $\left[T_n\right]^{e}$ such that Equation (B-23) becomes

$$\Delta\left\{F_E\right\}^{e}_{n+1} = \left[k_E\right]^{e}_{n} \Delta\left\{\delta\right\}^{e}_{n+1} \tag{B-24}$$

in which $\left[k_E\right]$ is the standard small displacement 'elastic' stiffness in global coordinates given by

$$\left[k_E\right]_n^e = \left[T_n\right]^{T\,e} \left[k'\right]^e \left[T_n\right]^e \quad . \tag{B-25}$$

Note that $\left[k_E\right]_n^e$ is in terms of quantities defined at the conclusion of step (n) or the beginning of step (n+1). The second term in Equation (B-21) represents the incremental nodal forces due to the 'Geometrical' effect of the change in the transformation matrix caused by the displacement increments and is defined as

$$\Delta\left\{F_G\right\}_{n+1}^e = \left[\Delta T_{n+1}\right]^{T\,e} \left\{F_n'\right\}^e \quad . \tag{B-26}$$

Since $\left[T\right]^T$ is a function of the displacements, for small displacement increments $\left[\Delta T\right]^T$ can be written as

$$\left[\Delta\ T_{n+1}\right]^{T\,e} = \frac{\partial\left[T_n\right]^{T\,e}}{\partial\left\{\delta\right\}^e} \Delta\left\{\delta\right\}_{n+1}^e \quad . \tag{B-27}$$

Substituting Equation (B-27) into (B-26) and rearranging the order, $\Delta\left\{F_G\right\}_{n+1}^e$ can be expressed as

$$\Delta\left\{F_G\right\}_{n+1}^e = \left[k_G\right]_n^e \Delta\left\{\delta\right\}_{n+1}^e \tag{B-28}$$

in which $\left[k_G\right]_n^e$ is the 'Geometrical' stiffness of the element in global coordinates. This stiffness is evidently a function of the <u>total</u>, local nodal forces $\left\{F_n'\right\}^e$ existing prior to step (n+1) and of the partial derivatives of the transformation matrix, $\left[T_n\right]$.

Thus, for small increments the change of internal element forces during the incremental step (n+1) can be obtained as

$$\Delta\left\{F\right\}^{e}_{n+1} = \left[\left[k_E\right]^{e}_{n} + \left[k_G\right]^{e}_{n}\right]\Delta\left\{\delta\right\}^{e}_{n+1} \qquad \text{(B-29)}$$

where Equations (B-21), (B-24), and (B-28) have been combined. This defines the desired 'incremental' stiffness $\left[k\right]^{e}_{n+1}$ in Equation (B-15) as

$$\left[k\right]^{e}_{n+1} = \left[k_E\right]^{e}_{n} + \left[k_G\right]^{e}_{n} \; . \qquad \text{(B-30)}$$

Hence, the solution of the assembly of all the elements is accomplished in the usual manner as if the stiffness of each element were simply a sum of the standard small displacement 'elastic' stiffness $\left[k_E\right]^{e}_{n}$ and the 'geometrical' stiffness $\left[k_G\right]^{e}_{n}$. The nonlinear problem has thus been reduced to a sequence of linear solutions. The increments in displacements, forces, and stresses are added to the previous values to give an up-to-date account of deformation as the load is increased incrementally.

The following can be considered an algorithm for the linear-incremental approach:

During step (n) an incremental load vector $\Delta\left\{R\right\}_n$ was applied to the assembled structure to yield the incremental displacements $\Delta\left\{\delta\right\}_n$. For each element of the structure in equilibrium at the conclusion of step (n) —

(i) Determine the new local coordinate transformation matrices corresponding to the updated nodal locations.

(ii) Calculate the incremental nodal forces resulting from the displacements in step (n). These forces, when added to the previous values, define the totals at the end of step (n). The total nodal forces in local coordinate components are needed to define the 'geometrical' stiffness for step (n+1).

(iii) Calculate the incremental ('elastic' plus 'geometric') stiffness in global coordinates, based on the configuration at the conclusion of step (n).

(iv) Repeat steps (i), (ii), and (iii) for all elements and assemble the global stiffness matrix for the entire structure, $\left[k \right]_{n+1}$.

(v) Apply the loading increment $\Delta \left\{ R \right\}_{n+1}$ to the assembled structure and calculate the resulting displacement increments $\Delta \left\{ \delta \right\}_{n+1}$ by solution of the simultaneous displacement equations of equilibrium

$$\Delta \left\{ R \right\}_{n+1} = \left[k \right]_{n+1} \Delta \left\{ \delta \right\}_{n+1} \quad . \tag{B-31}$$

(vi) Compute the incremental strains and stresses.

(vii) Update nodal coordinate locations.

(viii) The above steps are repeated until the entire loading has been applied.

In a previous section the reduction of large displacement shell problems to the analysis of the geometrically nonlinear large displacement problem in thin plates was discussed. In applying the linear-incremental approach to these problems, the displacements and hence displacement gradients per step can be reduced to the level such that

'plate bending' and 'in-plane' behavior are uncoupled. Hence in the following sections, the 'elastic' stiffness of the thin triangular element will be obtained in local coordinates by adding the independent bending and membrane stiffnesses suitable for small displacements. This stiffness will then be transformed to global orientation. The 'geometrical' stiffness will be derived in global coordinates and added to the global 'elastic' stiffness to form the total incremental stiffness. Matrix assembly and solution of the resulting displacement equations of equilibrium will then be described.

C. SMALL DISPLACEMENT FORMULATION

The most critical step in the finite element formulation is the evaluation of the stiffness properties of the individual elements. The element properties, including the stiffness, will be evaluated first in local coordinates and then transformed to global orientation via the standard transformation law.

It is assumed that the triangular elements are interconnected only at their corner (nodal) points. Thus, the element stiffness represents the forces at these nodal points resulting from unit displacements of the nodal points. Two types of element stiffness are considered for the flat-plate idealization in shell analysis; plate bending stiffness which accounts for displacements and rotations out of the element plane, and in-plane (membrane) stiffness which relates forces and displacements in the plane of the element. As noted in section B, there is no coupling between bending and in-plane behavior for small displacements. Therefore it will be convenient to consider the triangular element in bending and in plane stress separately

and then combine the resulting stiffnesses.

In Figure 3 a typical triangular element is illustrated showing the local coordinate system considered. Also shown are the displacements* and associated forces for the separated bending and in-plane actions in local coordinates. The choice of local coordinate directions is such that for a typical element with nodes i, j, k the x' and y' axes are in the middle-surface plane of the element. The x' axis is chosen along the edge i-j, positive in the direction i→j. The y' axis is perpendicular to the x' axis and chosen to pass through node k. The z axis is orthogonal to x' and y' and therefore to the plane of the element (assumed to be of uniform thickness) with direction defined by the right-hand rule. For uniformity, nodal points i, j, k will be chosen in a counterclockwise fashion when viewing from the exterior of the shell so that z' will always point outward.

1. 'PLATE BENDING' FORMULATION (Local Coordinates)

(a) DISPLACEMENT FUNCTIONS

For plate bending, the state of deformation is given uniquely by the lateral displacement $\tilde{w}'$* of the 'middle plane' of the plate. In accordance with compatibility requirements, on the interfaces between elements, it is necessary to impose continuity not only on $\tilde{w}'$ but also on its derivatives. This is to ensure that the plate

---

*For the finite element analysis in this section, the assumed displacement functions and resulting nodal displacements are all for points on the middle surface. Hence the subscript (o) is dropped for convenience. Since all the quantities of interest are for a characteristic element 'e', the superscript (e) is also dropped. In addition, since all forces and displacements are understood to be small incremental values, the del (Δ) is dropped.

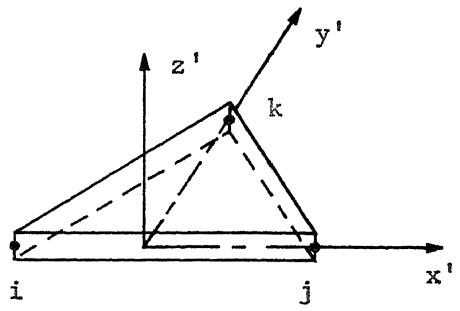

(a)

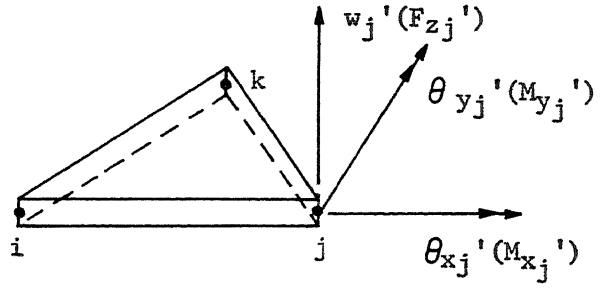

'Plate Bending' Displacements and Forces

(b)

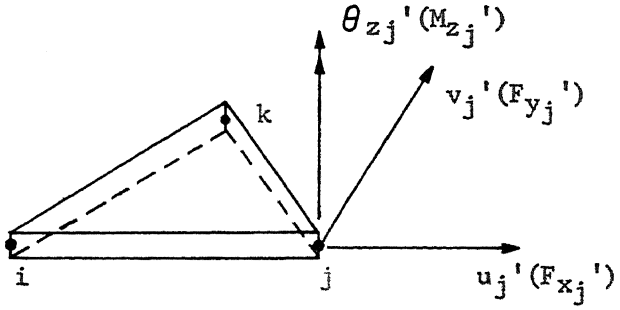

'Membrane' Displacements and Forces

Figure 3. A Typical Element Subject to 'Plate Bending' and 'Membrane' Actions in Local Coordinates.

remains continuous and does not 'kink.' (Note that in the limit as the number of flat-plate elements is increased, the idealization of a curved shell by these elements brings adjacent elements into the same plane). In finite element analysis of thin-plate bending, it is thus convenient to consider three degrees of freedom per node. These are given by the nodal displacement of the middle surface in the z' direction (w_j') and the rotations of the normal to the middle surface about the x' and y' axes, θ_{x_j}' and θ_{y_j}', respectively (see Figure 3(a)). The rotation terms are obviously identical to the slopes of $\tilde{w}'$ (except for sign). That is

$$\tilde{\theta}_{x}' = \frac{\partial \tilde{w}'}{\partial y'}$$
$$\tilde{\theta}_{y}' = -\frac{\partial \tilde{w}'}{\partial x'} \quad . \tag{C-1}$$

Hence in the bending formulation, the three degrees of freedom per node with three associated generalized forces (a force and two moments) are given for node 'i' as

---

*In the following, a tilde ($\sim$) will be used to indicate a quantity which is a function of the coordinates to distinguish it from the corresponding nodal quantities.

$$\left\{ \delta_i^{b'} \right\}^* = \begin{Bmatrix} w_i' \\ \theta_{x_i}' \\ \theta_{y_i}' \end{Bmatrix}$$

$$\left\{ F_i^{b'} \right\} = \begin{Bmatrix} F_{z_i}' \\ M_{x_i}' \\ M_{y_i}' \end{Bmatrix} . \qquad \text{(C-2)}$$

In an attempt to satisfy the aforementioned continuity requirements for bending displacements, the bending formulation adopted is that of Reference (16). Accordingly, a different displacement expansion is selected for each of the two subregions created by the previously chosen local axes system as shown in Figure 4. For inter-element compatibility, $\tilde{w}'$ must be a cubic function and the normal slope of $\tilde{w}'$ must vary linearly on the boundaries of the element. Choosing a complete cubic expansion in x' and y' for each subregion, eliminating the term x'^2y' by requiring a linearly varying normal slope along i-j, and deleting two parameters by requiring the normal slope to vary linearly along sides i-k and j-k gives the normal displacement expansions for subregions (1) and (2) as

$$\begin{aligned} \tilde{w}'^{(m)**} = {} & \alpha_1 + \alpha_2 x' + \alpha_3 y' + \alpha_4^{(m)} x'^2 + \alpha_5 x'y' \\ & + \alpha_6 y'^2 + (t^{(m)} x'^3 + x'y'^2)\,\alpha_8 \\ & + (r^{(m)} x'^3 + y'^3)\,\alpha_9 \end{aligned} \qquad \text{(C-3)}$$

---

*The superscript 'b' denotes those quantities associated with the bending formulation.

**The superscript in parentheses denotes for which subregion the quantity applies.

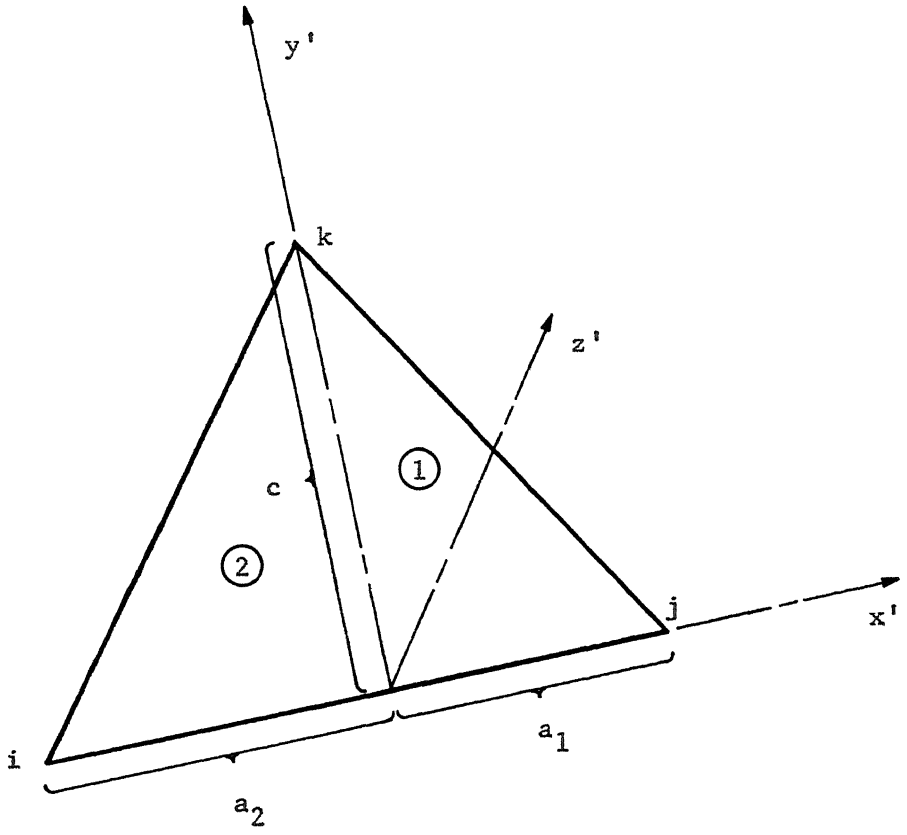

Figure 4. Element Subregions and Associated Dimensions.

with m = 1,2. The α's are constants to be determined in terms of nodal quantities. The terms $t^{(m)}$ and $r^{(m)}$ are given by

$$t^{(m)} = \frac{1}{3}\left[2 - \left(\frac{c}{a_m}\right)^2\right]$$
$$r^{(1)} = -\frac{c}{a_1}, \quad r^{(2)} = \frac{c}{a_2} \qquad m = 1,2 \qquad \text{(C-4)}$$

with dimensions a_1, a_2, and c defined in Figure 4. The nine α coefficients in Equation (C-3) can be written in terms of the element's nine degrees of freedom (three for each node) by substituting appropriate coordinates into the expressions for $\tilde{w}'$ and its derivatives as defined in Equations (C-1) and (C-3). Performing this substitution yields the element bending displacement vector

$$\left\{\delta^{b'}\right\} = \begin{Bmatrix} \delta_i^{b'} \\ \delta_j^{b'} \\ \delta_k^{b'} \end{Bmatrix} = \left[C1\right]\left\{\alpha\right\} \qquad \text{(C-5)}$$

where

$$\left\{\alpha\right\}^T = \left[\alpha_1, \alpha_2, \alpha_3, \alpha_4{}^{(1)}, \alpha_4{}^{(2)}, \alpha_5, \alpha_6, \alpha_8, \alpha_9\right] \qquad \text{(C-6)}$$

and $\left[C1\right]$ is given in Appendix I. Equation (C-5) can be solved for $\left\{\alpha\right\}$ to yield

$$\left\{\alpha\right\} = \left[C1\right]^{-1}\left\{\delta^{b'}\right\} . \qquad \text{(C-7)}$$

---

*The superscript in parentheses denotes for which subregion the quantity applies.

Also, Equation (C-3) can be written in the form

$$\tilde{w}'^{(m)} = \left[\tilde{P}\right]^{(m)} \left\{\alpha\right\} \quad , \quad m = 1,2 \tag{C-8}$$

where

$$\begin{aligned}\left[\tilde{P}\right]^{(1)} = &\left[1,\ x',\ y',\ x'^2,\ 0,\ x'y',\ y'^2,\ t^{(1)}x'^3\right. \\ &\left. + x'y'^2,\ r^{(1)}x'^3 + y'^3\right] \\ \left[\tilde{P}\right]^{(2)} = &\left[1,\ x',\ y',\ 0,\ x'^2,\ x'y',\ y'^2,\ t^{(2)}x'^3\right. \\ &\left. + x'y'^2,\ r^{(2)}x'^3 + y'^3\right] .\end{aligned} \tag{C-9}$$

The element displacement functions (C-3) have been chosen to satisfy the requirements of normal slope continuity along edges between adjacent elements and throughout the interior of the element. The transverse displacement $\tilde{w}'$ satisfies continuity requirements along edges i-k and j-k but not along i-j. However, this incomplete fulfillment of compatibility requirements is not significant as demonstrated by the excellent results obtained with this element for small displacement plate bending in Reference (16).

(b) STRAIN AND STRESS MATRICES

In accordance with classical thin-plate theory, the variation in stresses and strains on lines normal to the plane of the plate is prescribed to be linear. Accordingly, the normals to the middle plane remain straight, unstrained, and normal to the middle surface after deformation (i.e. $\tilde{\epsilon}_{z'} = \tilde{\gamma}_{x'z'} = \tilde{\gamma}_{y'z'} = 0$). This is the classical Kirchoff assumption discussed in section B.

The actual strains in any plane at a distance z' from the middle plane can be described in terms of the three curvatures of $\tilde{w}'$. These

generalized strains (curvatures) are defined as

$$\left\{\tilde{K}^{b'}\right\} = \begin{Bmatrix} \tilde{K}_{x'}{}^{b} \\ \tilde{K}_{y'}{}^{b} \\ \tilde{K}_{x'y'}{}^{b} \end{Bmatrix} = \begin{Bmatrix} -\dfrac{\partial^2 \tilde{w}'}{\partial x'^2} \\ -\dfrac{\partial^2 \tilde{w}'}{\partial y'^2} \\ -2\dfrac{\partial^2 \tilde{w}'}{\partial x' \partial y'} \end{Bmatrix} . \qquad \text{(C-10)}$$

The 'engineering' strains at a distance z' from the middle plane can be expressed in terms of the generalized strains as

$$\begin{Bmatrix} \tilde{\epsilon}_{x'}{}^{b} \\ \tilde{\epsilon}_{y'}{}^{b} \\ \tilde{\gamma}_{x'y'}{}^{b} \end{Bmatrix} = z' \left\{\tilde{K}^{b'}\right\} . \qquad \text{(C-11)}$$

Similarly, the actual stresses at a distance z' above the middle surface can be found in terms of the stress resultant internal moments. Using the familiar notation and referring to Figure 5, three such moments are defined at any point fixing the stresses throughout the thickness. These are $\tilde{M}_{x'}$, $\tilde{M}_{y'}$, and $\tilde{M}_{x'y'}$ which represent the resultants of stresses acting per unit distance x' or y'. Therefore, the generalized stresses are defined as

$$\left\{\tilde{M}^{b'}\right\} = \begin{Bmatrix} \tilde{M}_{x'}{}^{b} \\ \tilde{M}_{y'}{}^{b} \\ \tilde{M}_{x'y'}{}^{b} \end{Bmatrix} = \int_{-\frac{h}{2}}^{\frac{h}{2}} \begin{Bmatrix} \tilde{\sigma}_{x'}{}^{b} \\ \tilde{\sigma}_{y'}{}^{b} \\ \tilde{\tau}_{x'y'}{}^{b} \end{Bmatrix} z' \, dz' . \qquad \text{(C-12)}$$

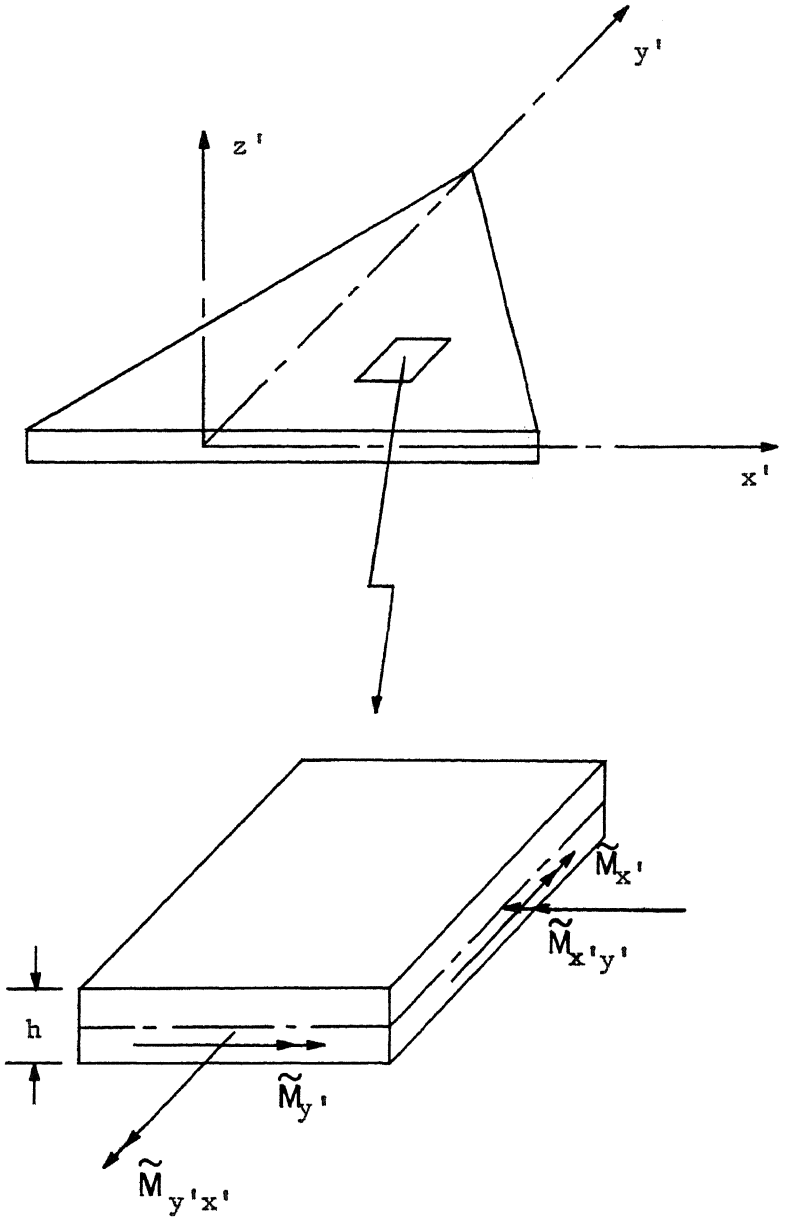

Figure 5. Stress Resultants for Plate Bending.

Corresponding to the engineering strains, the stresses at a distance z' from the middle surface can be expressed in terms of the generalized stresses as

$$\left\{\tilde{\sigma}^{b'}\right\} = \begin{Bmatrix} \tilde{\sigma}_{x'}{}^{b} \\ \tilde{\sigma}_{y'}{}^{b} \\ \tilde{\tau}_{x'y'}{}^{b} \end{Bmatrix} = \frac{12z'}{h^3}\left\{\tilde{M}^{b'}\right\} \qquad \text{(C-13)}$$

where 'h' is the thickness of the element. In general, the strains and stresses defined by Equations (C-11) and (C-13) are functions of x', y', and z'.

For subregions (1) and (2) (see Figure 4) the appropriate expression for $\tilde{w}'$ from Equation (C-8) can be differentiated according to Equation (C-10) to give the generalized strain matrices

$$\left\{\tilde{K}^{b'}\right\}^{(m)} = \left[\tilde{Q}\right]^{(m)}\left\{\alpha\right\} \quad , \; m = 1,2 \qquad \text{(C-14)}$$

in which $\left[\tilde{Q}\right]^{(m)}$, $m = 1,2$ are defined in Appendix I. Applying Equation (C-7), (C-14) can be written in terms of the nodal displacements as

$$\left\{\tilde{K}^{b'}\right\}^{(m)} = \left[\tilde{B}^{b}\right]^{(m)}\left\{\delta^{b'}\right\} \quad , \; m = 1,2 \qquad \text{(C-15)}$$

where

$$\left[\tilde{B}^{b}\right]^{(m)} = \left[\tilde{Q}\right]^{(m)}\left[C1\right]^{-1} \quad , \; m = 1,2 \; . \qquad \text{(C-16)}$$

Note: It can be shown that the assumed displacement functions given by Equation (C-3) permit possible constant strain states and include the rigid body modes. They thus satisfy the completeness requirements set forth in Chapter III.

(c) STRESS - STRAIN RELATION

The linear relationship between stress and strain for an isotropic, homogeneous, elastic plate without initial strain* is given on page 81 of Reference (17) as

$$\left\{ \tilde{M}^{b'} \right\} = \left[D^{b} \right] \left\{ \tilde{K}^{b'} \right\} \tag{C-17}$$

where the elasticity matrix is given by

$$\left[D^{b} \right] = \frac{Eh^3}{12(1-\nu^2)} \begin{bmatrix} 1 & \nu & 0 \\ \nu & 1 & 0 \\ 0 & 0 & \frac{1-\nu}{2} \end{bmatrix} \tag{C-18}$$

with E Young's modulus, h the thickness, and ν the Poisson's ratio. These relations for subregions (1) and (2) yield

$$\left\{ \tilde{M}^{b'} \right\}^{(m)} = \left[D^{b} \right] \left\{ \tilde{K}^{b'} \right\}^{(m)} , \; m = 1,2. \tag{C-19}$$

---

*Initial strains, that is strains caused by an initial lack of fit, temperature change, shrinkage, etc., have not been considered in this analysis. Their inclusion would introduce an initial strain matrix in Equation (C-17).

By utilizing Equations (C-13), (C-19), and (C-15) the stresses for subregions (1) and (2) can be written in terms of nodal displacements as

$$\left\{ \tilde{\sigma}^{b'} \right\}^{(m)} = \frac{12z'}{h^3} \left[D^b \right] \left[\tilde{B}^b \right]^{(m)} \left\{ \delta^{b'} \right\}, \quad m = 1,2. \tag{C-20}$$

This relation will be used later to calculate the stresses due to bending at nodes i, j, and k on the inner and outer surfaces ($z' = \mp \frac{h}{2}$).

(d) STIFFNESS MATRIX

The $\left[9 \times 9 \right]$ plate-bending stiffness matrix defined by

$$\begin{Bmatrix} F_i^{b'} \\ F_j^{b'} \\ F_k^{b'} \end{Bmatrix} = \left[k^{b'} \right] \begin{Bmatrix} \delta_i^{b'} \\ \delta_j^{b'} \\ \delta_k^{b'} \end{Bmatrix} \tag{C-21}$$

relates the local nodal forces to the corresponding nodal displacements (refer to Equation (C-2)) and is given by

$$\left[k^{b'} \right] = \int_A \left[\tilde{B}^b \right]^T \left[D^b \right] \left[\tilde{B}^b \right] dA \tag{C-22}$$

where A is the area of the middle surface and $\left[\tilde{B}^b \right]$ is defined in Equation (C-16). Recalling that $\left[\tilde{B}^b \right]^{(m)}$ is valid for subregion m, m = 1,2 the stiffness matrix may be rewritten as

$$\begin{aligned} \left[k^{b'} \right] = & \int_{A(1)} \left[\tilde{B}^b \right]^T (1) \left[D^b \right] \left[\tilde{B}^b \right] (1) \; dA(1) \\ & + \int_{A(2)} \left[\tilde{B}^b \right]^T (2) \left[D^b \right] \left[\tilde{B}^b \right] (2) \; dA(2) \end{aligned} \tag{C-23}$$

where $A^{(1)}$ and $A^{(2)}$ are the areas of subregions (1) and (2), respectively. Substituting Equation (C-16) into (C-23), the stiffness matrix for bending can be written as

$$\left[k^{b'}\right] = \left[\left[C1\right]^{-1}\right]^{T} \left[k^{b'}\right]^{(1,2)} \left[C1\right]^{-1} \tag{C-24}$$

where

$$\left[k^{b'}\right]^{(1,2)} = \left[k^{b'}\right]^{(1)} + \left[k^{b'}\right]^{(2)} \tag{C-25}$$

and

$$\left[k^{b'}\right]^{(m)} = \int_{A(m)} \left[\tilde{Q}\right]^{T(m)} \left[Db\right] \left[\tilde{Q}\right]^{(m)} dA^{(m)}, \qquad m = 1,2. \tag{C-26}$$

The matrices in Equation (C-26) have been integrated over the middle surface of the triangular element to yield the combined matrix $\left[k^{b'}\right]^{(1,2)}$ given in Appendix I.

The inverse of $\left[C1\right]$ will be obtained in the computer so that the bending stiffness can be calculated by performing the matrix multiplications in Equation (C-24). This stiffness matrix can then be partitioned and submatrices extracted according to

$$\left[k^{b'}\right] = \begin{bmatrix} k_{ii}^{b'} & k_{ij}^{b'} & k_{ik}^{b'} \\ k_{ji}^{b'} & k_{jj}^{b'} & k_{jk}^{b'} \\ k_{ki}^{b'} & k_{kj}^{b'} & k_{kk}^{b'} \end{bmatrix} \tag{C-27}$$

where the subscripts on each of the $\left[3 \times 3\right]$ bending submatrices correspond to the nodes i, j, k of the element.

2. 'IN - PLANE' FORMULATION (Local Coordinates)

(a) DISPLACEMENT FUNCTIONS

For the in-plane or membrane behavior of the thin triangular element in plane stress, the state of deformation is given uniquely by two in-plane components of nodal displacement $\tilde{u}'$ and $\tilde{v}'$ in the local x' and y' directions, respectively (see Figure 3 (b)). The rotation about the z' axis, $\tilde{\theta}_z$, must be small with respect to the local coordinate axes and for shell theory, negligible compared with other displacement components. Hence there are two degrees of freedom per node with two associated generalized forces given for a typical node 'i' as

$$\left\{\delta_i^{p'}\right\}^* = \begin{Bmatrix} u_i' \\ v_i' \end{Bmatrix} \qquad \left\{F_i^{p'}\right\} = \begin{Bmatrix} F_{xi}' \\ F_{yi}' \end{Bmatrix} . \tag{C-28}$$

If the displacement field is to be continuous between adjacent elements, which are is the same plane in the limit as the mesh size is reduced, it is necessary that each component of in-plane displacement vary in a linear manner along the sides of the element. Accordingly, a linear expansion in x' and y' is chosen for each of the in-plane displacements. Thus,

---

*The superscript 'p' denotes those quantities associated with the in-plane formulation.

$$\tilde{u}' = \beta_1 + \beta_2 x' + \beta_3 y'$$
$$\tilde{v}' = \beta_4 + \beta_5 x' + \beta_6 y' \qquad \text{(C-29)}$$

where the β's are constants to be determined in terms of nodal displacements. This can be accomplished by substituting the appropriate coordinates for nodes i, j, and k into Equation (C-29) and solving the six resulting simultaneous equations to yield

$$\{\beta\} = \begin{Bmatrix} \beta_1 \\ \beta_2 \\ \beta_3 \\ \beta_4 \\ \beta_5 \\ \beta_6 \end{Bmatrix} = [CP]\{\delta^{P'}\} \qquad \text{(C-30)}$$

where

$$\{\delta^{P'}\} = \begin{Bmatrix} \delta_i{}^{P'} \\ \delta_j{}^{P'} \\ \delta_k{}^{P'} \end{Bmatrix} \qquad \text{(C-31)}$$

is the element in-plane displacement vector and $[CP]$ is given in Appendix II. Equation (C-29) can now be written in the form

$$\tilde{u}' = [1\ x'\ y'\ 0\ 0\ 0]\{\beta\}$$
$$\tilde{v}' = [0\ 0\ 0\ 1\ x'\ y']\{\beta\} \quad . \qquad \text{(C-32)}$$

(b) STRAIN AND STRESS MATRICES

The total strain at any point within the element can be defined by its three engineering strain components which contribute to internal work. These generalized strains for in-plane action are defined as

$$\left\{\tilde{\epsilon}^{p'}\right\} = \begin{Bmatrix} \tilde{\epsilon}_{x'}{}^{p} \\ \tilde{\epsilon}_{y'}{}^{p} \\ \tilde{\gamma}_{x'y'}{}^{p} \end{Bmatrix} = \begin{Bmatrix} \dfrac{\partial \tilde{u}'}{\partial x'} \\ \dfrac{\partial \tilde{v}'}{\partial y'} \\ \dfrac{\partial \tilde{u}'}{\partial y'} + \dfrac{\partial \tilde{v}'}{\partial x'} \end{Bmatrix} . \qquad \text{(C-33)}$$

The above strain-displacement relations incorporate the assumption of small strains and small rotations such that second degree terms can be neglected. Differentiating the displacement expansions in Equation (C-32) according to (C-33) and employing (C-30), the engineering strains can be expressed in terms of nodal displacements as

$$\left\{\epsilon^{p'}\right\} = \left[B^{p}\right] \left\{\delta^{p'}\right\} \qquad \text{(C-34)}$$

with $\left[B^{p}\right]$ defined in Appendix II. Since the terms of $\left[B^{p}\right]$ are constants associated with the element geometry, the assumed displacement expansions define a constant strain state throughout the element. Hence the tilde ($\sim$) is not needed in Equation (C-34). It can be shown that the assumed displacement functions also provide zero strain states for the possible rigid body motions. Thus the completeness requirements set forth in Chapter III are satisfied.

For the assumed plane stress condition, the non-zero stresses corresponding to the generalized strains in Equation (C-33) are defined as

$$\left\{ \tilde{\sigma}^{P'} \right\} = \begin{Bmatrix} \tilde{\sigma}_{x'}{}^{P} \\ \tilde{\sigma}_{y'}{}^{P} \\ \tilde{\tau}_{x'y'}{}^{P} \end{Bmatrix} . \tag{C-35}$$

(c) STRESS - STRAIN RELATION

For plane stress in an isotropic material without initial strains, the stress-strain relation is given by

$$\left\{ \sigma^{P'} \right\} = \left[D^{P} \right] \left\{ \epsilon^{P'} \right\} \tag{C-36}$$

with the elasticity matrix defined as

$$\left[D^{P} \right] = \frac{E}{1-\nu^2} \begin{bmatrix} 1 & \nu & 0 \\ \nu & 1 & 0 \\ 0 & 0 & \frac{1-\nu}{2} \end{bmatrix} . \tag{C-37}$$

Since a condition of constant strain and hence stress exists throughout the triangular element, Equation (C-36) defined the stress state for nodes i, j, and k due to the in-plane action at both the inner and outer surfaces ($z' = \mp \frac{h}{2}$). Thus, again the tilde has been omitted.

(d) STIFFNESS MATRIX

The $\left[6 \text{ X } 6\right]$ in-plane stiffness matrix defined in the equation

$$\begin{Bmatrix} F_i^{p'} \\ F_j^{p'} \\ F_k^{p'} \end{Bmatrix} = \left[k^{p'}\right] \begin{Bmatrix} \delta_i^{p'} \\ \delta_j^{p'} \\ \delta_k^{p'} \end{Bmatrix} \tag{C-38}$$

relates the local nodal forces to the corresponding nodal displacements (refer to Equation (C-28)). This stiffness matrix is defined by

$$\left[k^{p'}\right] = \int_V \left[B^p\right]^T \left[D^p\right]\left[B^p\right] \, dV \tag{C-39}$$

where V is the volume of the element of uniform thickness h. The matrix $\left[B^p\right]$, given in Appendix II, can be partitioned in the form

$$\left[B^p\right] = \left[B_i^p \;\; B_j^p \;\; B_k^p\right] \quad . \tag{C-40}$$

Substituting Equation (C-40) into (C-39), performing the matrix multiplications indicated, and realizing that the matrices within the integral contain only constant terms, the $\left[6 \text{ X } 6\right]$ in-plane stiffness matrix of the element is given by

$$\left[k^{p'}\right] = \begin{bmatrix} k_{ii}^{p'} & k_{ij}^{p'} & k_{ik}^{p'} \\ k_{ji}^{p'} & k_{jj}^{p'} & k_{jk}^{p'} \\ k_{ki}^{p'} & k_{kj}^{p'} & k_{kk}^{p'} \end{bmatrix} \tag{C-41}$$

where the $\left[2 \times 2\right]$ submatrices are defined as

$$\left[k_{rs}{}^{P\prime}\right] = \left[B_r{}^{P}\right]^{T} \left[D^{P}\right] \left[B_s{}^{P}\right] \frac{c\, h(a_1 + a_2)}{2} \qquad \text{(C-42)}$$

with r, s = i, j, k.

3. COMBINED 'BENDING' AND 'IN - PLANE' FORMULATIONS (Local Coordinates)

(a) THE 'ELASTIC' STIFFNESS

Before combining the 'plate bending' and 'in-plane' formulations, it is important to note two facts. The first, that the displacements prescribed for 'in-plane' action do not affect the 'plate bending' deformations and vice versa. This is due to the assumption of small displacements. Second, the rotation $\theta_z{}'$ does not enter into either mode of deformation. It is convenient to include it now and associate with it a fictitious couple $M_z{}'$. The fact that it does not enter as a displacement variable can be accounted for by inserting appropriate zeros in the stiffness matrix. Its inclusion is advantageous when transformation to global orientation and assembly are considered.

Redefining the combined nodal displacements due to bending and in-plane actions as

$$\left\{\delta_i{}'\right\} = \begin{Bmatrix} u_i{}' \\ v_i{}' \\ w_i{}' \\ \theta_{x_i}{}' \\ \theta_{y_i}{}' \\ \theta_{z_i}{}' \end{Bmatrix} \qquad \text{(C-43)}$$

and the appropriate generalized 'forces' as

$$\left\{F_i'\right\} = \begin{Bmatrix} F_{x_i}' \\ F_{y_i}' \\ F_{z_i}' \\ M_{x_i}' \\ M_{y_i}' \\ M_{z_i}' \end{Bmatrix} \tag{C-44}$$

it is now possible to write

$$\begin{Bmatrix} F_i' \\ F_j' \\ F_k' \end{Bmatrix} = \left[k'\right] \begin{Bmatrix} \delta_i' \\ \delta_j' \\ \delta_k' \end{Bmatrix} \tag{C-45}$$

or

$$\left\{F'\right\} = \left[k'\right] \left\{\delta'\right\} \quad . \tag{C-46}$$

The $\left[18 \text{ X } 18\right]$ combined 'elastic' stiffness matrix in local coordinates is given in partitioned form as

$$\left[k'\right] = \begin{bmatrix} k_{ii}' & k_{ij}' & k_{ik}' \\ k_{ji}' & k_{jj}' & k_{jk}' \\ k_{ki}' & k_{kj}' & k_{kk}' \end{bmatrix} \tag{C-47}$$

and can be shown to be made up of the submatrices

$$\left[k_{rs}'\right] = \left[\begin{array}{cc|ccc|c} & & 0 & 0 & 0 & 0 \\ \multicolumn{2}{c|}{\left[k_{rs}^{p'}\right]} & 0 & 0 & 0 & 0 \\ \hline 0 & 0 & & & & 0 \\ 0 & 0 & \multicolumn{3}{c|}{\left[k_{rs}^{b'}\right]} & 0 \\ 0 & 0 & & & & 0 \\ \hline 0 & 0 & 0 & 0 & 0 & 0 \end{array}\right] \qquad \text{(C-48)}$$

r, s = i, j, k, if it is noted that

$$\left\{\delta_i'\right\} = \left\{\begin{array}{c} \delta_i^{p'} \\ \delta_i^{b'} \\ \theta_{z_i}' \end{array}\right\} \quad . \qquad \text{(C-49)}$$

The submatrices $\left[k_{rs}^{b'}\right]$ and $\left[k_{rs}^{p'}\right]$ are given in Equations (C-27) and (C-42), respectively.

(b) COMBINED STRESSES

The stresses at the inner and outer surfaces of the element due to combined bending and in-plane actions are the ones of interest. The extremum stress levels are obviously there since the bending stresses reach their maximum magnitudes there and are zero at the middle surface, while the in-plane stresses are uniform throughout the thickness. This fact is illustrated in Figure 6 for the stress component σ_x'.

For all three nodes, the stresses for in-plane action are given by Equation (C-35) throughout the thickness and need no further discussion. The bending stresses on the inner and outer surfaces are given in Equation (C-20) by substituting $z' = -\frac{h}{2}$ & $\frac{h}{2}$, respectively. Nodes i and j are

clearly in subregions (2) and (1), respectively (see Figure 4). Node k being common to both subregions, it is convenient to calculate the bending stresses for subregions (1) and (2) at the node and to average the two. For all three nodes then, the bending stresses are

$$\begin{aligned}\left\{\sigma_i^{b'}\right\} &= \left\{\sigma_i^{b'}\right\}^{(2)} \\ \left\{\sigma_j^{b'}\right\} &= \left\{\sigma_j^{b'}\right\}^{(1)} \\ \left\{\sigma_k^{b'}\right\} &= \tfrac{1}{2}\left\{\sigma_k^{b'}\right\}^{(1)} + \tfrac{1}{2}\left\{\sigma_k^{b'}\right\}^{(2)} .\end{aligned} \tag{C-50}$$

Thus the combined stresses due to bending and in-plane actions at $z' = \mp \frac{h}{2}$ are given by

$$\left\{\sigma_m'\right\}_{\mp\frac{h}{2}} = \left\{\sigma_m^{b'}\right\}_{\mp\frac{h}{2}} + \left\{\sigma^{p'}\right\} \quad , \; m = i,\ j,\ k \tag{C-51}$$

where the stresses due to bending are defined by Equation (C-50) upon specifying $z' = \mp h/2$.

The stress components $\sigma_{x'}$, $\sigma_{y'}$, and $\tau_{x'y'}$, defined for nodes i, j, and k by Equation (C-51), will be used to calculate the principal stresses at both the inner and outer surfaces. For all elements having a particular node in common, these principal stresses will be averaged. This averaging effect will tend to reduce the error introduced when the smoothly-curved shell surface was approximated by one made up of flat triangular plates, each of which may be in a slightly different plane when joined at a particular node.

The principal stress equations, being the standard ones for two-dimensional stress, will not be included here.

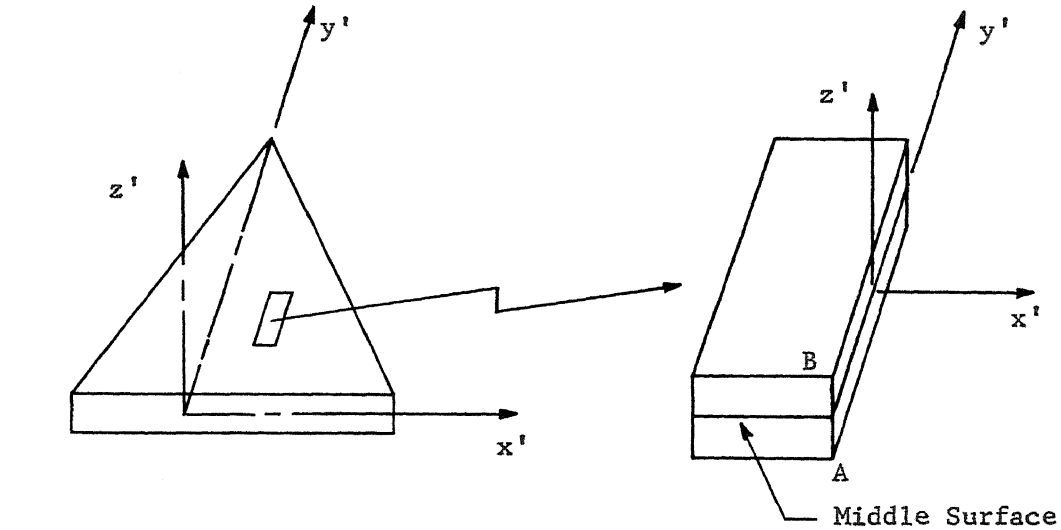

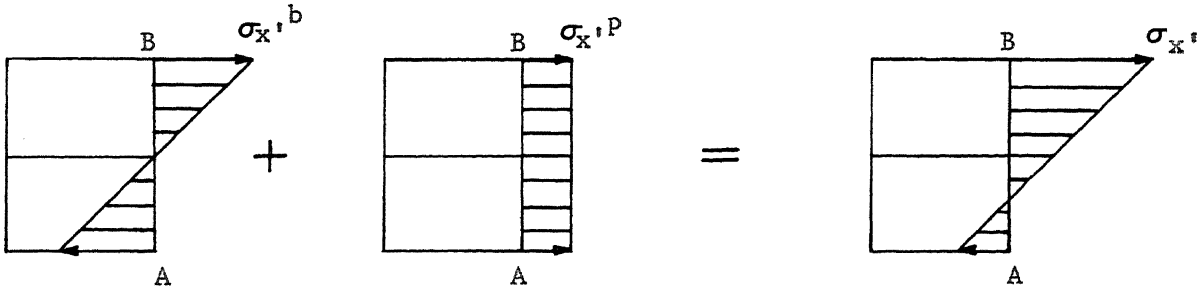

Bending Stress In-Plane Stress Combined Stress

Figure 6. Combined Stress due to Bending and In-Plane Actions.

4. GLOBAL TRANSFORMATION

The element small displacement 'elastic' stiffness matrix derived in the previous sections used a system of local coordinates. Transformation to a global coordinate system, common to all the elements, will be necessary for assembly. In addition, it will be more convenient to specify the element nodes by their global coordinates and to establish from these the local coordinates, thus requiring an inverse transformation.

The two systems of coordinates have been shown previously in Figure 1. The nodal displacement and force components in local coordinates transform from the global system by a matrix $[L]$ as

$$\begin{Bmatrix} \delta_i' \end{Bmatrix} = \begin{bmatrix} L \end{bmatrix} \begin{Bmatrix} \delta_i \end{Bmatrix}$$
$$\begin{Bmatrix} F_i' \end{Bmatrix} = \begin{bmatrix} L \end{bmatrix} \begin{Bmatrix} F_i \end{Bmatrix} \qquad \text{(C-52)}$$

with the force and displacement vectors defined in Equations (A-1) through (A-4). The transformation matrix $[L]$ is defined as

$$\begin{bmatrix} L \end{bmatrix} = \begin{bmatrix} \lambda & 0 \\ 0 & \lambda \end{bmatrix} \qquad \text{(C-53)}$$

with $[\lambda]$ a $[3 \times 3]$ matrix of direction cosines of angles formed between the two sets of axes. $[\lambda]$ is derived in Appendix III.

For the entire set of forces acting on the nodes of an element it is now possible to write

$$\begin{Bmatrix} \delta' \end{Bmatrix} = \begin{bmatrix} T \end{bmatrix} \begin{Bmatrix} \delta \end{Bmatrix}$$
$$\begin{Bmatrix} F' \end{Bmatrix} = \begin{bmatrix} T \end{bmatrix} \begin{Bmatrix} F \end{Bmatrix} \quad .$$

By the rules of orthogonal transformation the 'elastic' stiffness matrix of the element in global coordinates becomes

$$\left[k_E\right] = \left[T\right]^T \left[k'\right] \left[T\right] \tag{C-55}$$

with $\left[k'\right]$ given in Equation (C-47). In the above relations, $\left[T\right]$ is given by

$$\left[T\right] = \begin{bmatrix} L & 0 & 0 \\ 0 & L & 0 \\ 0 & 0 & L \end{bmatrix} . \tag{C-56}$$

A typical submatrix $\left[k_{rs_E}\right]$ of the partitioned $\left[18 \text{ X } 18\right]$ 'elastic' stiffness matrix

$$\left[k_E\right] = \begin{bmatrix} k_{ii_E} & k_{ij_E} & k_{ik_E} \\ k_{ji_E} & k_{jj_E} & k_{jk_E} \\ k_{ki_E} & k_{kj_E} & k_{kk_E} \end{bmatrix} \tag{C-57}$$

can be shown to be

$$\left[k_{rs_E}\right] = \left[L\right]^T \left[k_{rs}'\right] \left[L\right] \tag{C-58}$$

in which $\left[k_{rs}'\right]$ is defined in Equation (C-48).

D. LARGE DISPLACEMENT FORMULATION

1. THE 'GEOMETRICAL' STIFFNESS

In section B, the concept of the 'geometrical' stiffness matrix for use in the linear-incremental approach was outlined. In step (n+1), the incremental global nodal forces for an element, due to the geometrical effect of large displacements, were given in Equation (B-26) as

$$\Delta \left\{ F_G \right\}^e_{n+1} = \left[\Delta T_{n+1} \right]^{Te} \left\{ F_n' \right\}^{e*} \tag{D-1}$$

in which

$$\left[\Delta T \right]^{Te} = \begin{bmatrix} \Delta T_{1,1} & \Delta T_{2,1} & \cdots & \Delta T_{18,1} \\ \Delta T_{1,2} & \Delta T_{2,2} & \cdots & \Delta T_{18,2} \\ \cdot & & & \cdot \\ \cdot & & & \cdot \\ \cdot & & & \cdot \\ \Delta T_{1,18} & \Delta T_{2,18} & \cdots & \Delta T_{18,18} \end{bmatrix}^e . \tag{D-2}$$

For small steps, the terms in Equation (D-2) being functions of nodal coordinates can be expanded in the form

---

*In this and the following sections the superscript (e) denotes those matrices associated with a particular element as opposed to those associated with the overall assembled system.

$$\Delta T^{e}_{r,s} = \frac{\partial T^{e}_{r,s}}{\partial x_i} \Delta u_i + \frac{\partial T^{e}_{r,s}}{\partial y_i} \Delta v_i + \cdots + \frac{\partial T^{e}_{r,s}}{\partial x_j} \Delta u_j + \cdots \quad \text{(D-3)}$$

Expanding each of the terms in Equation (D-2) in this manner, $\Delta \left\{ F_G \right\}^{e}_{n+1}$ can be rearranged to the form

$$\Delta \left\{ F_G \right\}^{e}_{n+1} = \left[k_G \right]^{e}_{n} \Delta \left\{ \delta \right\}^{e}_{n+1} \quad \text{(D-4)}$$

where the 'geometrical' stiffness is given by

$$\left\{ k_G \right\}^{e}_{n} = \left[T_n \right]^{Te} \begin{bmatrix} F_{ii}' & F_{ii}' & F_{ii}' \\ F_{jj}' & F_{jj}' & F_{jj}' \\ F_{kk}' & F_{kk}' & F_{kk}' \end{bmatrix}_n^{e} \begin{bmatrix} \frac{\partial}{\partial \delta_i} & 0 & 0 \\ 0 & \frac{\partial}{\partial \delta_j} & 0 \\ 0 & 0 & \frac{\partial}{\partial \delta_k} \end{bmatrix}_n \quad \text{(D-5)}$$

in which

$$\left[F_{mm}' \right]^{e}_{n} = \left[F_m' \; F_m' \; F_m' \; F_m' \; F_m' \; F_m' \right]^{e}_{n} \quad , \; m = i, \; j, \; k \quad \text{(D-6)}$$

and $\left[F_m' \right]$ is given in Equation (C-44). Also, the matrix of partial derivative operators with respect to the element's nodal coordinates is defined as

$$\left[\frac{\partial}{\partial \delta_m} \right]_n = \begin{bmatrix} \frac{\partial}{\partial x_m} & 0 & 0 & 0 & 0 & 0 \\ 0 & \frac{\partial}{\partial y_m} & 0 & 0 & 0 & 0 \\ 0 & 0 & \frac{\partial}{\partial z_m} & 0 & 0 & 0 \\ 0 & 0 & 0 & 0 & 0 & 0 \\ 0 & 0 & 0 & 0 & 0 & 0 \\ 0 & 0 & 0 & 0 & 0 & 0 \end{bmatrix}_n \quad , \; m = i, \; j, \; k. \quad \text{(D-7)}$$

Partial derivatives with respect to the angular coordinates do not appear in Equation (D-7) since they are zero in (D-3). This is so because the transformation matrix derived in Appendix III is formulated in terms of x, y, and z coordinates of the element's nodal points. The subscript (n) can be dropped in the following with the understanding that all terms are referenced to the equilibrium configuration existing prior to the new loading step.

By employing Equation (C-56) and performing the multiplications indicated in (D-5), a typical submatrix of the partitioned $\left[18 \text{ X } 18\right]$ 'geometrical' stiffness matrix

$$\left[k_G\right]^e = \begin{bmatrix} k_{ii_G} & k_{ij_G} & k_{ik_G} \\ k_{ji_G} & k_{jj_G} & k_{jk_G} \\ k_{ki_G} & k_{kj_G} & k_{kk_G} \end{bmatrix}^e \tag{D-8}$$

becomes

$$\left[k_{rs_G}\right]^e = \left[L\right]^{T_e} \left[F_{rr'}\right]^e \left[\frac{\partial}{\partial \delta_s}\right] \tag{D-7}$$

with all matrices previously defined. All that remains is to perform the matrix multiplications called for in Equation (D-7) with the understanding that the partial derivatives apply to the direction cosines in the transformation matrix. The resulting elements of this 'geometrical' stiffness submatrix are too lengthy to present here. For the interested reader, they are included in Appendix IV.

One further comment is appropriate here. The 'geometrical' stiffness, as derived from a purely geometrical standpoint, is non-symmetric. This is unfortunate as will be pointed out later when problem solutions are discussed.

2. THE INCREMENTAL STIFFNESS

As previously described in section B, the element stiffness desired for use in the linear-incremental approach, the incremental stiffness, is merely the sum of the previously derived 'elastic' and 'geometrical' stiffnesses. Thus a typical submatrix of the partitioned $\left[18 \text{ X } 18\right]$ incremental stiffness matrix

$$\left[k\right]^e = \begin{bmatrix} k_{ii} & k_{ij} & k_{ik} \\ k_{ji} & k_{jj} & k_{jk} \\ k_{ki} & k_{kj} & k_{kk} \end{bmatrix}^e \tag{D-8}$$

becomes

$$\left[k_{rs}\right]^e = \left[k_{rs_E}\right]^e + \left[k_{rs_G}\right]^e \tag{D-9}$$

with $\left[k_{rs_E}\right]^e$ and $\left[k_{rs_G}\right]^e$ given in Equations (C-58) and (D-7), respectively. Although the 'elastic' stiffness matrix is symmetric, the non-symmetric 'geometrical' stiffness renders the incremental stiffness matrix of the element non-symmetric.

3. MATRIX ASSEMBLY

For a shell with 'P' nodal points there are 6P degrees of freedom giving a structural stiffness matrix of dimensions $\left[6P \text{ X } 6P\right]$. The $\left[18 \text{ X } 18\right]$ incremental stiffness matrices for all elements of the structure must be evaluated as outlined in the previous sections and superimposed to form the overall structural stiffness.

For element 'e' with nodes i, j, and k, the terms in the $\left[6 \text{ X } 6\right]$ incremental stiffness submatrix $\left[k_{rs}\right]^e$, given by Equation (D-9), are added into the respective locations

$$\begin{bmatrix} k_{6r-5,6s-5}, & k_{6r-5,6s-4}, & k_{6r-5,6s-3}, & k_{6r-5,6s-2}, & k_{6r-5,6s-1}, & k_{6r-5,6s} \\ k_{6r-4,6s-5}, & k_{6r-4,6s-4}, & k_{6r-4,6s-3}, & k_{6r-4,6s-2}, & k_{6r-4,6s-1}, & k_{6r-4,6s} \\ k_{6r-3,6s-5}, & k_{6r-3,6s-4}, & k_{6r-3,6s-3}, & k_{6r-3,6s-2}, & k_{6r-3,6s-1}, & k_{6r-3,6s} \\ k_{6r-2,6s-5}, & k_{6r-2,6s-4}, & k_{6r-2,6s-3}, & k_{6r-2,6s-2}, & k_{6r-2,6s-1}, & k_{6r-2,6s} \\ k_{6r-1,6s-5}, & k_{6r-1,6s-4}, & k_{6r-1,6s-3}, & k_{6r-1,6s-2}, & k_{6r-1,6s-1}, & k_{6r-1,6s} \\ k_{6r,6s-5}, & k_{6r,6s-4}, & k_{6r,6s-3}, & k_{6r,6s-2}, & k_{6r,6s-1}, & k_{6r,6s} \end{bmatrix} \quad \text{(D-10)}$$

in the overall stiffness matrix $\left[k \right]$. The stiffness components due to all the elements will be superimposed (added) in this manner.

As outlined in section B, the assembled stiffness matrix is then used in calculating the incremental displacements due to an incremental application of the loading according to the linear relation

$$\Delta\left\{ R \right\} = \left[k \right] \Delta\left\{ \delta \right\} \quad \text{(D-11)}$$

with $\left[k \right]$ the assembled structural stiffness described above.

CHAPTER V

METHOD OF SOLUTION

The large displacement finite element analysis using the linear-incremental approach requires the repeated formulation and solution of a large number of simultaneous equations expressed in Equation (D-11) of Chapter IV. To accomplish this, a computer program was written for and executed on the IBM 360 machine at the University of Missouri at Rolla Computer Center. The program was limited in capacity to maintain an in-core solution. Effort was concentrated on developing an operating program which could produce solutions to the problems under consideration. However, no effort was devoted to optimizing numerical computations. A listing of the program together with a brief description of the input format and output data is given in Appendix V.

A. PROGRAM OUTLINE

An outline of the program for the linear-incremental approach is shown in Figures 7 and 8. For problems in which extremely large displacements are expected which would require an excessive number of increments to maintain linear geometrical relationships for each step, an alternate iteration option is provided.

1. ALTERNATE ITERATION OPTION

For each loading increment in the program using iteration in conjunction with the incremental approach, a specified number of iterations are employed to cause the displacement state to converge to the equilibrium solution corresponding to the total applied loading thus far.

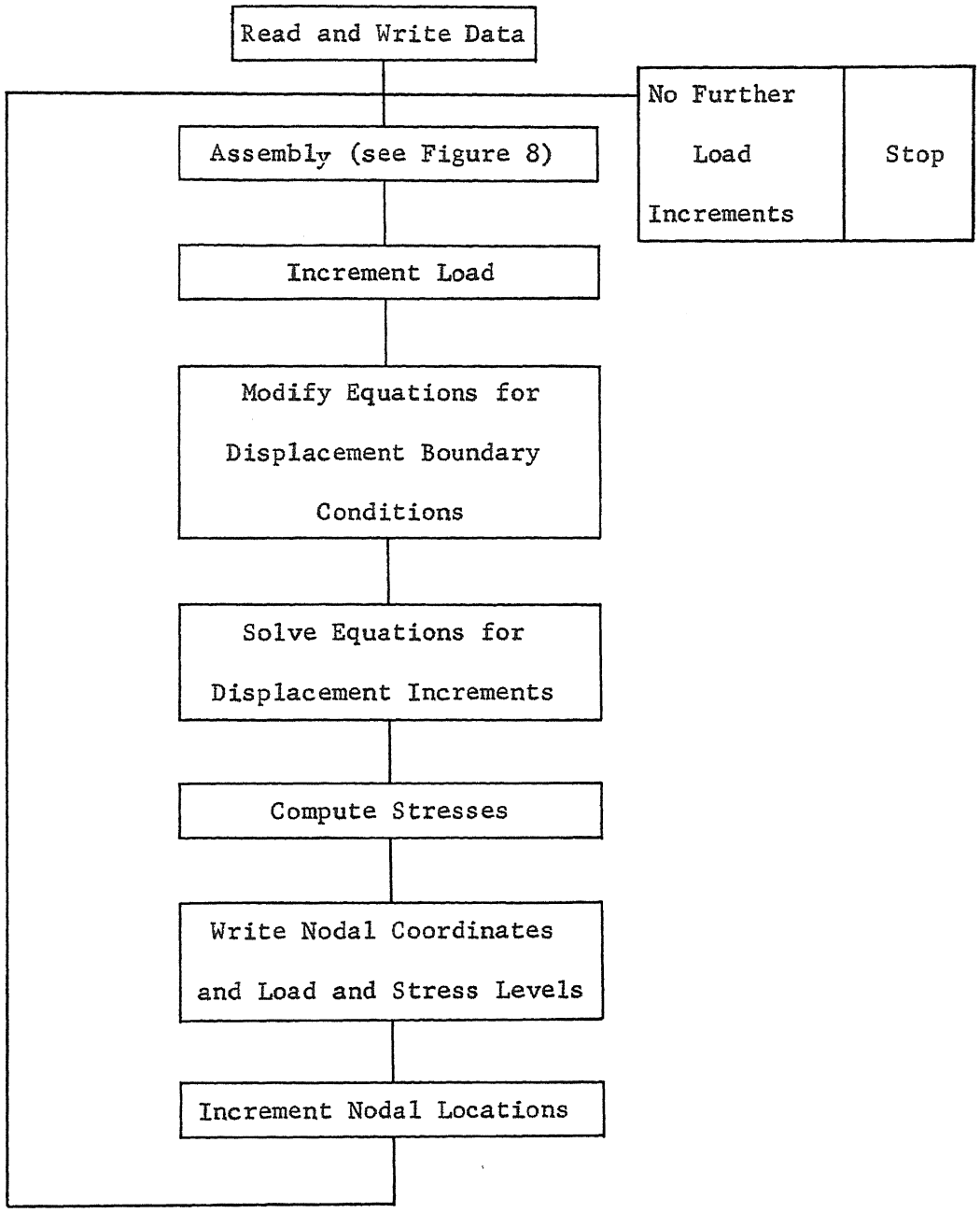

Figure 7. Program Outline for Linear-Incremental Approach

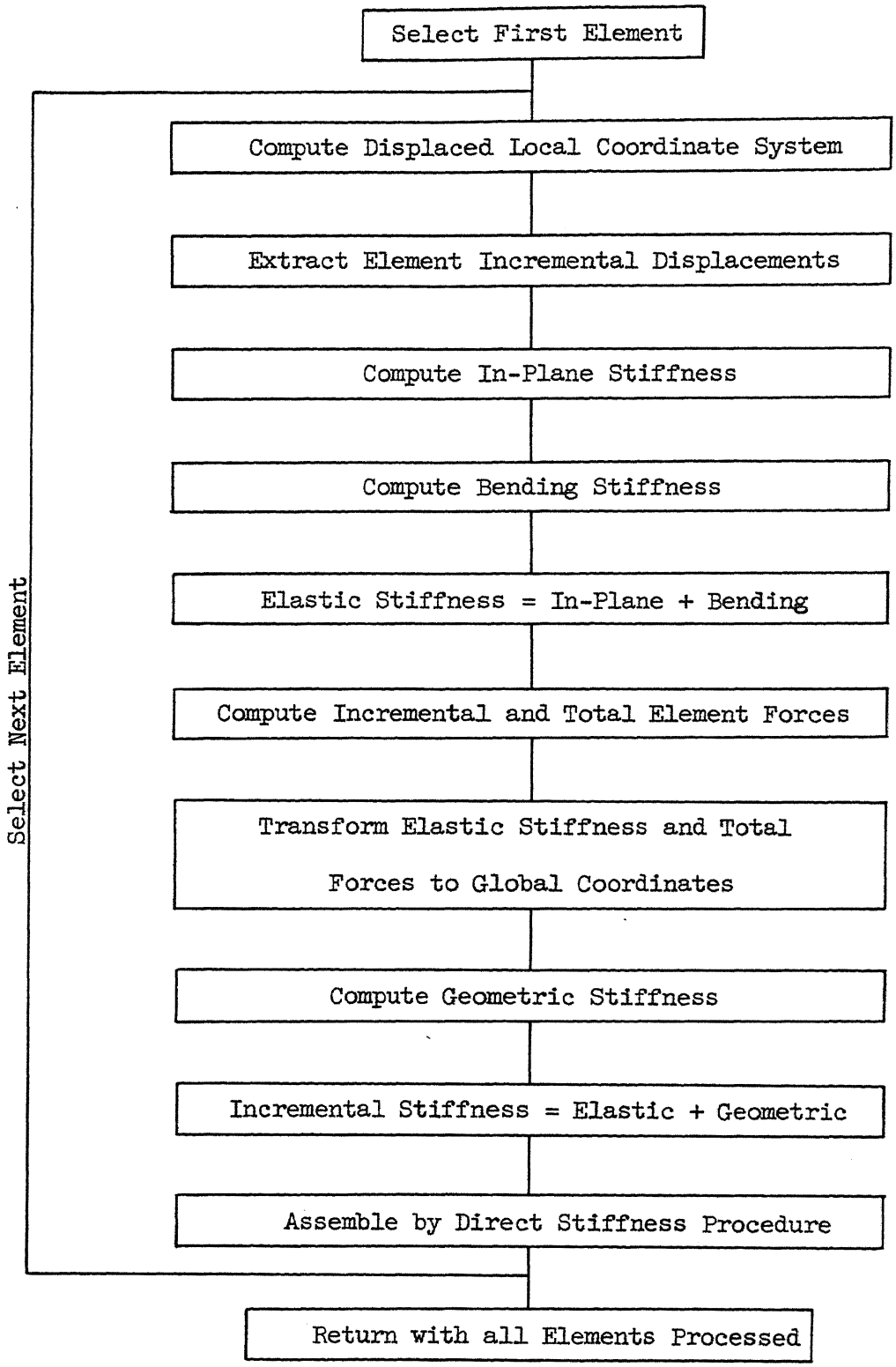

Figure 8. Outline of Stiffness Assembly

This is accomplished by seeking a force balance between applied loading and the nodal forces reacting the displacement state. Each iterative step is identical to the normal incremental step as shown in Figure 7 except that:

(i) The difference between the applied loads and the total reaction forces, the unbalanced loads, are determined and applied as the loading increment.

(ii) The applied load level is left unchanged.

(iii) The 'write' statement is skipped.

B. COMPUTATIONAL EFFORT

The principal shortcoming of the 'geometrical' stiffness approach to large displacement problems is the computational effort involved. As pointed out previously, the non-symmetrical 'geometrical' stiffness renders the incremental stiffness non-symmetrical. This necessitates handling the entire stiffness matrix and precludes usage of the more efficient routines developed for inverting symmetrical, positive definite matrices. Moreover, each incremental (or iterative) step requires the complete solution of a small deflection problem. For these reasons in addition to the fact that no effort was made to optimize computations, machine running time was understandably large.

The total solution time depends of course on the number of elements employed and even more significantly on the number of nodal points which determines the dimensions of the assembled stiffness matrix to be handled. Computation time rose disproportionately fast with an increased number of nodes and to a lesser extent with an increased number of elements. The

program was limited to treating 21 nodal points and 30 elements. Symmetry was taken advantage of wherever possible.

Some typical times for solutions on the IBM 360 for problems carried out in this investigation are as follows:

SOLUTION PROCEDURE	NUMBER OF NODES	SOLUTION TIME PER ELEMENT PER STEP (ITERATE) IN SECONDS
Incremental	9	5.6
	15	8.1
Incremental & Iteration	20	13.7

CHAPTER VI

VERIFICATION OF METHOD

The large displacement finite element method presented was applied to four large deflection thin-plate problems for which experimental data or numerical solutions were available in the literature. This was done in order to demonstrate the validity and versatility of the method. The problems treated include various boundary conditions with concentrated as well as distributed loading. In this investigation distributed loadings were replaced by statically equivalent, concentrated nodal loads according to assigned nodal areas. To facilitate the assignment of areas, uniform grids were employed.

A. SIMPLY SUPPORTED SQUARE PLATE; EDGE DISPLACEMENT = 0

The first example presented is that of a simply supported 10 inch square plate, 0.04 inches thick, subjected to a uniform normal pressure of 1.837 psi and edge forces such that edge displacements (but not rotations) on all sides are zero. The results can be compared with those obtained by Levy (18). Levy solved the von Karman equations (see Equations (B-14) in Chapter IV) consisting of two coupled equations in which the dependent variables were the stress function and the out-of-plane displacement. The dependent variables were approximated by a truncated trigonometric series and convergence was examined as more terms were added.

The plate was assumed to have a modulus of elasticity of 27.6×10^6 psi and a Poisson's ratio of 0.316.* The uniform loading was applied in 40 increments without iteration.

The center deflection vs. loading plot is shown in Figure 9.** A maximum central deflection of nearly twice the thickness (h) was attained. The stiffening of the plate with increasing deflection is indicated by the decreasing slope of the curve. Thus a given load increase would yield a much smaller displacement increment at a higher load level than near the unloaded state. This stiffening effect is due to the fact that appreciable lateral displacement induces a stretching of the middle surface thus stiffening the plate against further deflection. The deflection path for small deflection theory illustrates that such theory is applicable only for deflections less than ¼ the thickness. This example is obviously one of large deflections. Note the excellent agreement with Levy's solution.

The plot of principal stresses due to combined bending and in-plane actions is shown in Figure 10. The agreement of stresses with Levy's solution is not as good as for deflections. The principal stresses plotted are average values at the nodes.

The effect of grid size on the accuracy of the finite element model is shown in Figure 11 for this same problem. The square plate was idealized with 32, 72, and 128 element uniform meshes.

---

*The value of 0.316 was chosen to agree with that in Levy's solution. Levy was primarily interested in Aluminum and adopted this value.

**In the following figures, unless stated otherwise, the results of only every other loading step are shown for clarity.

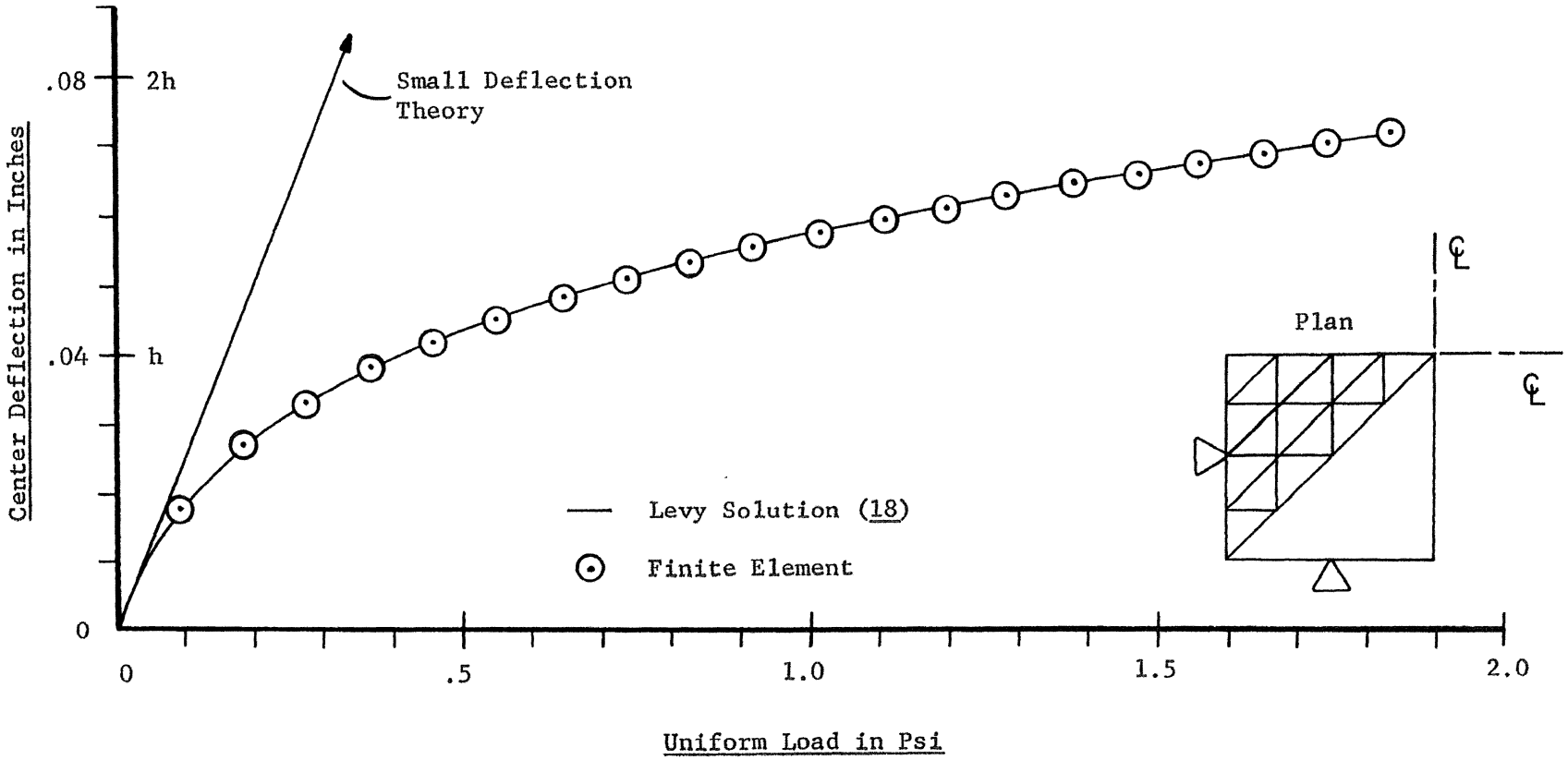

Figure 9. Load-Deflection of Simply Supported Square Plate; Edge Displacement = 0.

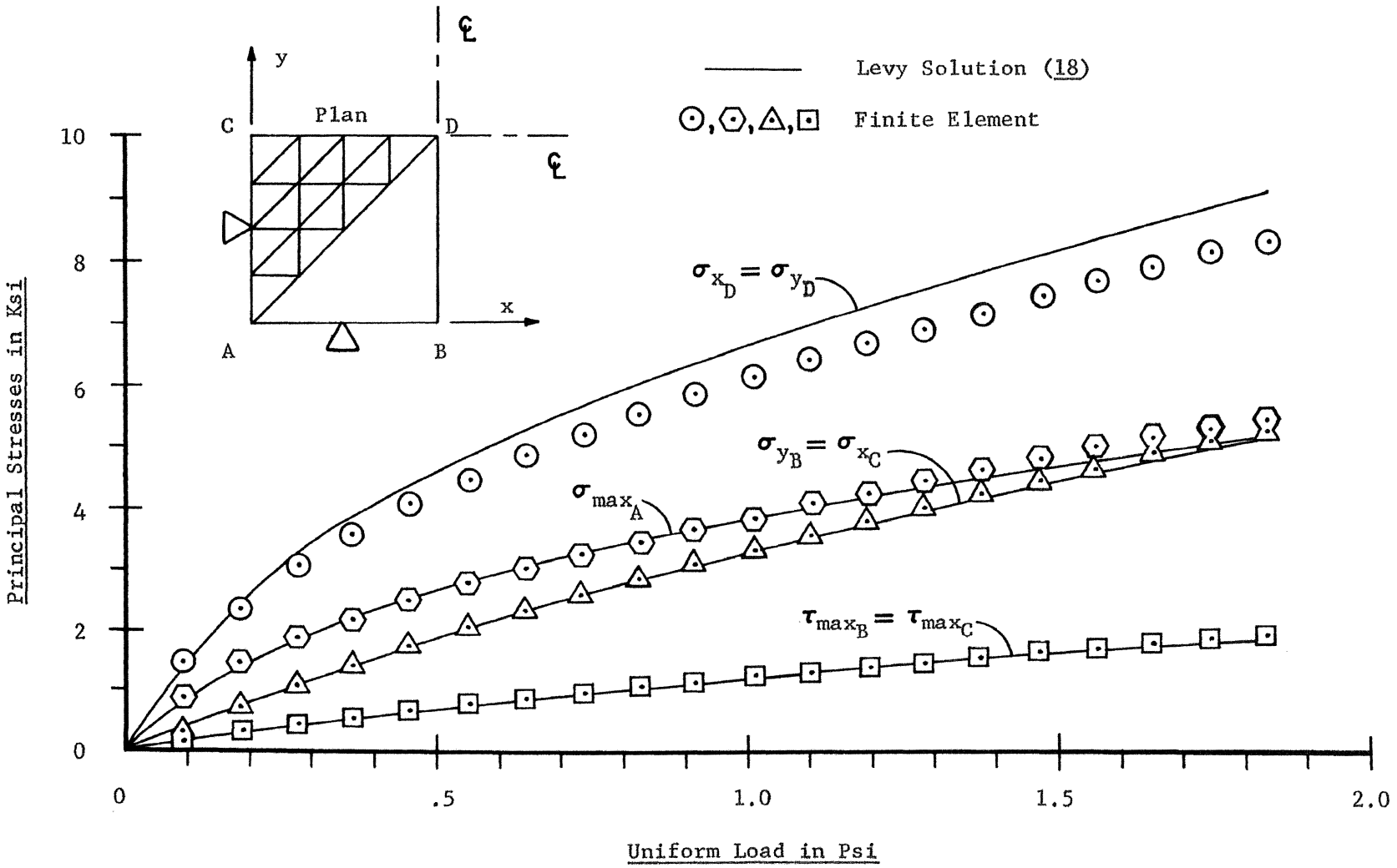

Figure 10. Principal Stresses in Simply Supported Square Plate; Edge Displacement = 0.

For the center deflection, the convergence of the solution with refined mesh size is evident. This indicates that the displacement discontinuities introduced in the finite element model diminish as the mesh size is reduced.

To illustrate the step size effect, the above example was also solved using a uniform grid of 128 elements but with the loading applied in 10, 20, and 40 equal steps. The effect of step size on the solution for the center deflection is shown in Figure 12. Each loading step is included in the figure. The step size is evidently critical in obtaining an accurate solution. This is particularly true for the first few loading steps because the true deflection curve is more nonlinear there. The fact that the displacements for each loading step are the solution of a linear problem is illustrated in that for each loading application, the first step falls on the curve for linear, small deflection theory. A large first step would obviously yield displacements greater than those for the true solution.

B. SIMPLY SUPPORTED SQUARE PLATE;

EDGE COMPRESSION = 0

A frequently encountered boundary condition is that of a simple support which constrains the edges to remain straight, prevents normal edge displacement, but allows unrestricted motion in the plane of the undeformed plate. A 6 inch square plate, 0.05 inches thick, subject to the above boundary conditions on all edges, was loaded with a uniform normal pressure of 60.28 psi. The loading was applied in 20 increments with no iteration. The plate was assumed to have a modulus of elasticity of 25.0×10^6 psi and a Poisson's ratio of 0.316.

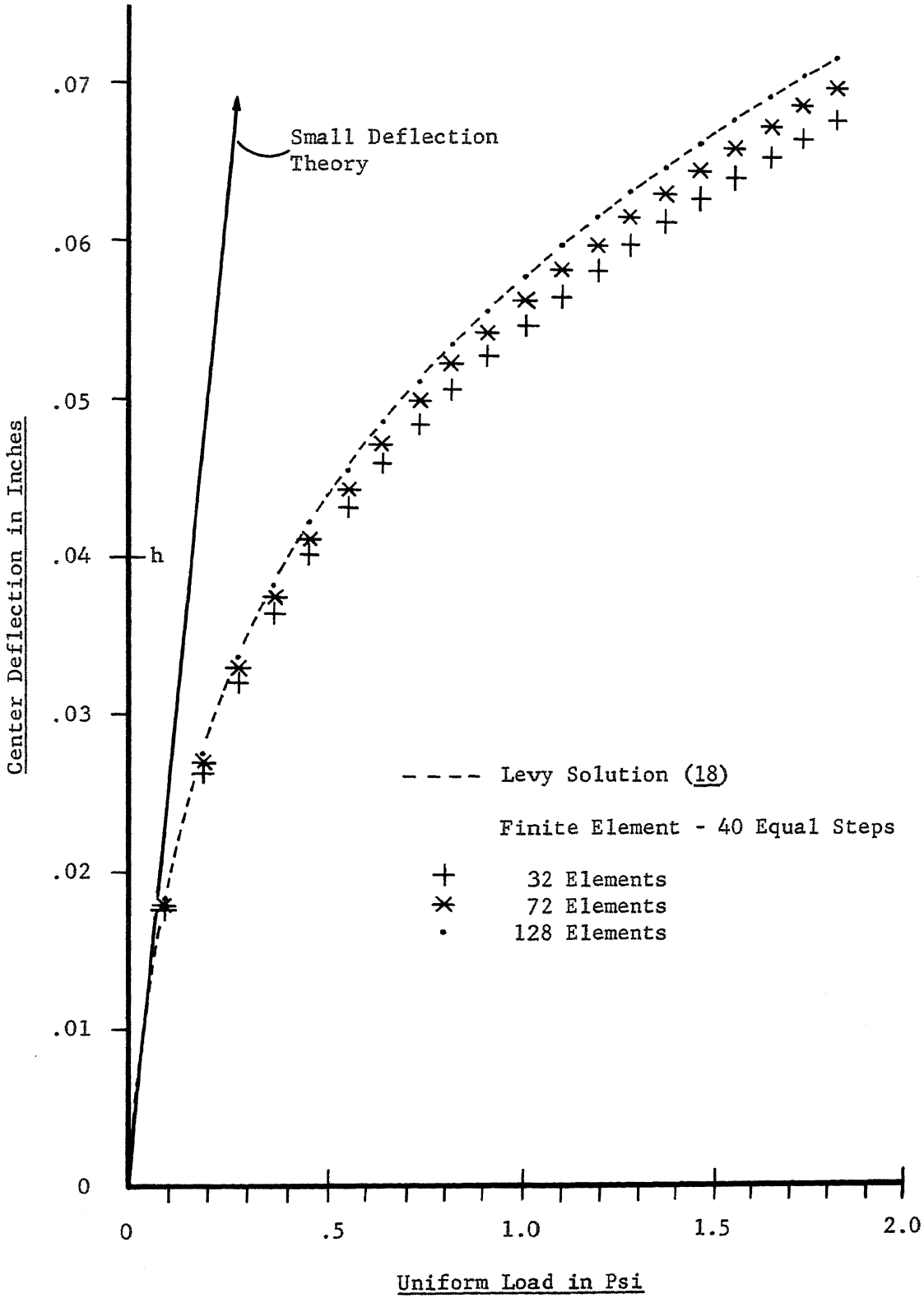

Figure 11. Grid Size Effect on Load-Deflection of Simply Supported Square Plate; Edge Displacement=0.

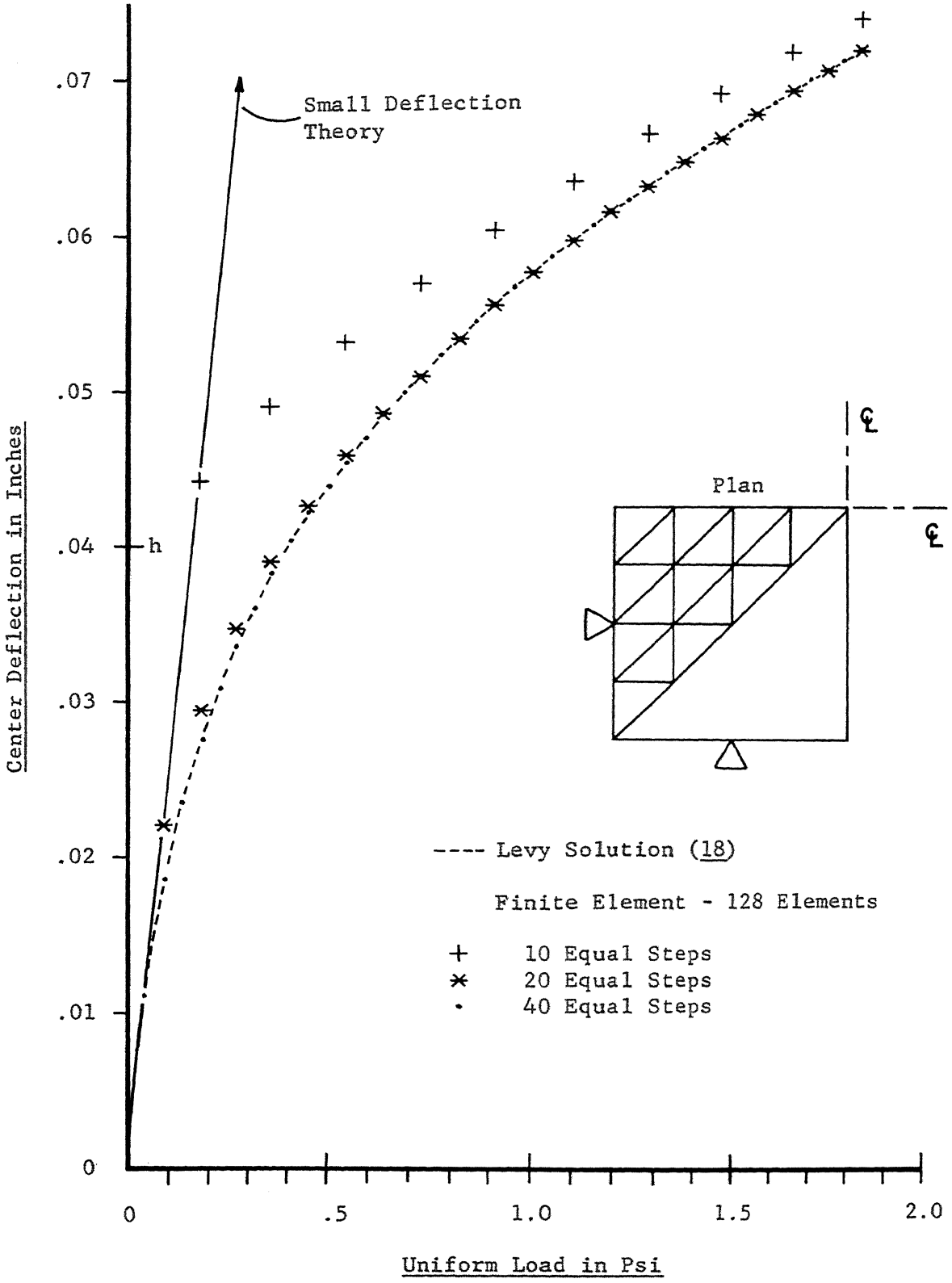

Figure 12. Step Size Effect on Load-Deflection of Simply Supported Square Plate; Edge Displacement=0.

In Figure 13 the finite element solution is compared to the solution by Levy (18) in a plot of center deflection vs. loading. The agreement with Levy's solution is reasonable. A center deflection of nearly 3 times the thickness was attained. This is evidently well into the large deflection range. The stiffening of the plate with increased loading is again appreciable.

The comparison of the finite element principal stress solution to Levy's solution is given in Figure 14. The stress results from the finite element approach are evidently in error even though the displacements agreed reasonably well. A discussion of this discrepancy will be given in section E.

C. RIGIDLY CLAMPED SQUARE PLATE

The deflection of a plate subject to large normal loads depends to a large extent on the edge boundary conditions imposed. As suggested previously, any constraint which promotes stretching of the middle surface for accompanying lateral deflection enhances the plate stiffness. Hence a rigidly clamped edge can be expected to have a significant stiffening effect for deflections larger than 1/4 to 1/3 the plate thickness.

An 8 inch rigidly clamped square plate, 0.05 inches thick, was considered as the next example. A uniform normal pressure of 16.0 psi was applied in 40 incremental steps. Iteration was not employed. A modulus of elasticity of 27.6×10^6 psi and a Poisson's ratio of 0.3 were chosen as material properties. The results can be compared to those obtained by Timoshenko (17). Timoshenko obtained an approximate solution to this problem by use of the energy method. Displacement

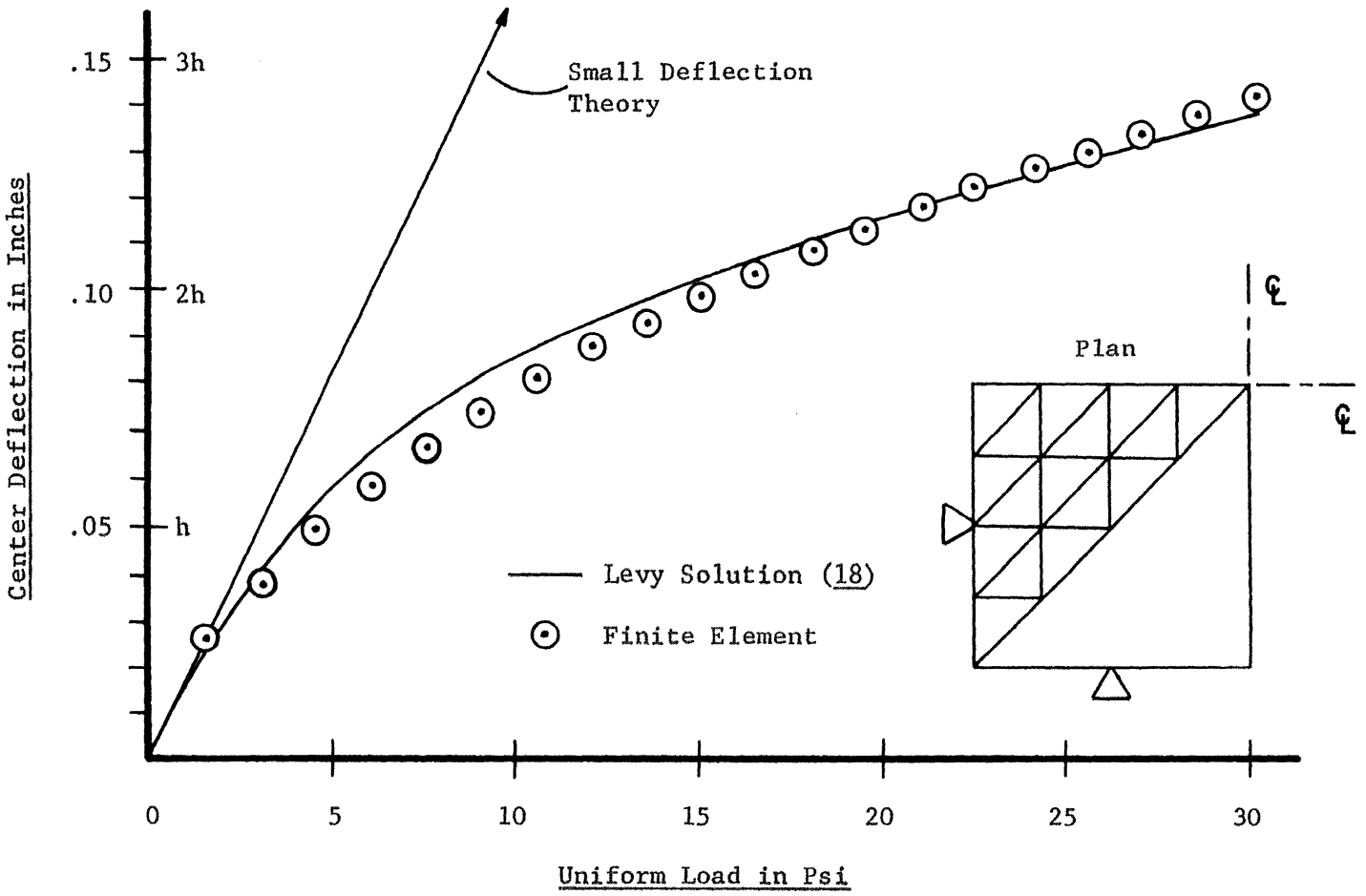

Figure 13. Load-Deflection of Simply Supported Square Plate; Edge Compression = 0.

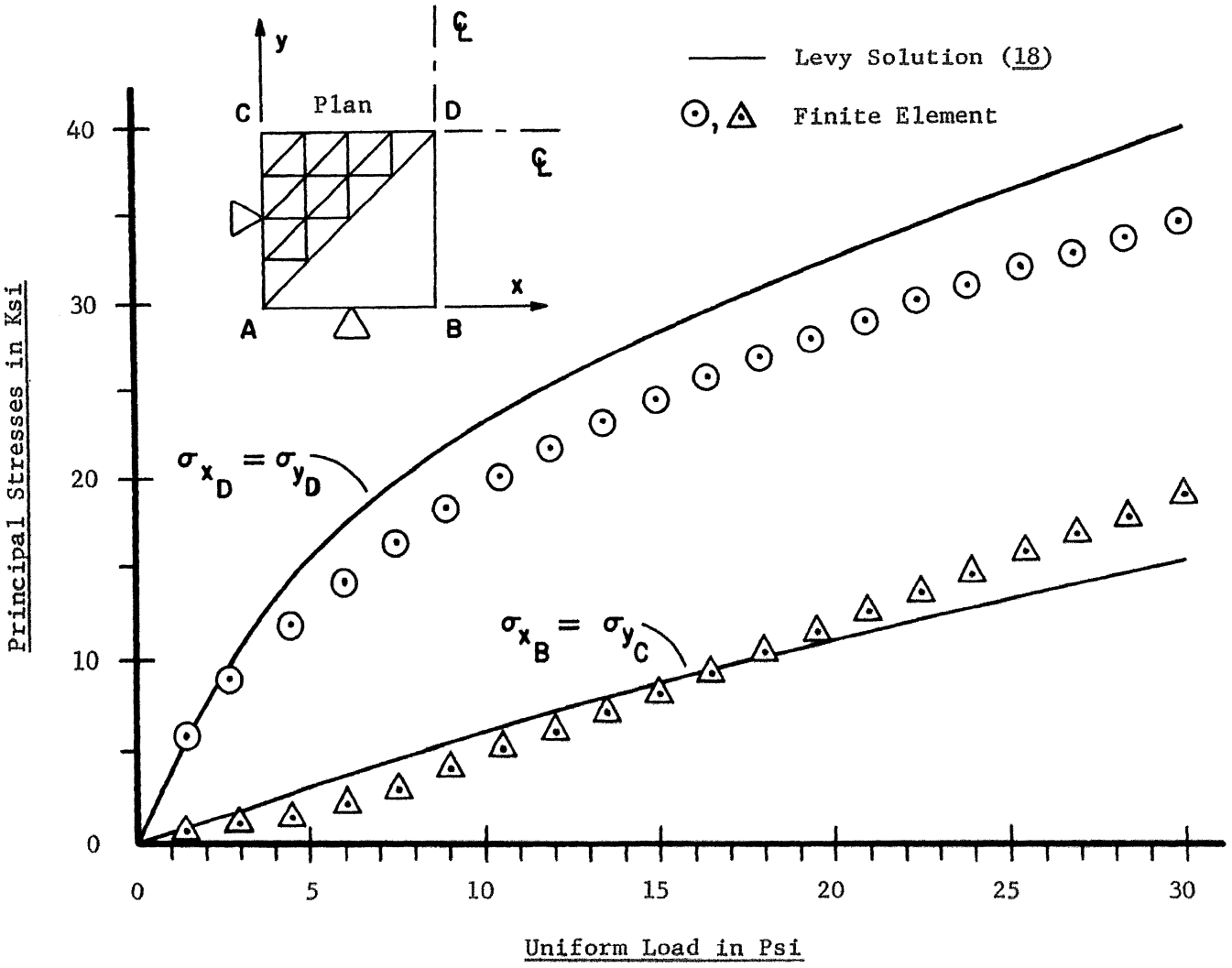

Figure 14. Principal Stresses in Simply Supported Square Plate; Edge Compression = 0.

functions for the in-plane and out-of-plane displacements were chosen to satisfy the clamped boundary conditions. The energy equations from the principal of virtual displacements were solved by the method of successive approximations.

The center deflection vs. loading plot is given in Figure 15. The stiffening effect of the induced membrane forces with increased loading is again evident. The deflections from the finite element solution were slightly larger than those obtained by Timoshenko, but uniformly so throughout the loading. A number of finer mesh and smaller step size combinations were employed to obtain finite element results all of which essentially agreed with those in Figure 15. This would suggest that the finite element solution may be more accurate than the results obtained by Timoshenko. Timoshenko indicated that his solution was only an approximate one due to the use of a finite number of constants in the displacement expansions.

Figure 16 shows a plot of principal stress vs. load. The finite element stress was less than Timoshenko's solution by approximately 5% throughout the loading. Timoshenko indicated that his calculated stresses were in error on the safe side (i.e., too large) lending added confidence to the finite element solution.

D. Cantilevered Plate

In order to compare the finite element method to published experimental results, a problem with extreme nonlinearities was selected.

A cantilevered plate, 0.0194 inches thick and rigidly clamped on one edge to expose a 6 inch square surface, was subjected to a concentrated corner load of 1.544 pounds. A modulus of elasticity of 18.5×10^6

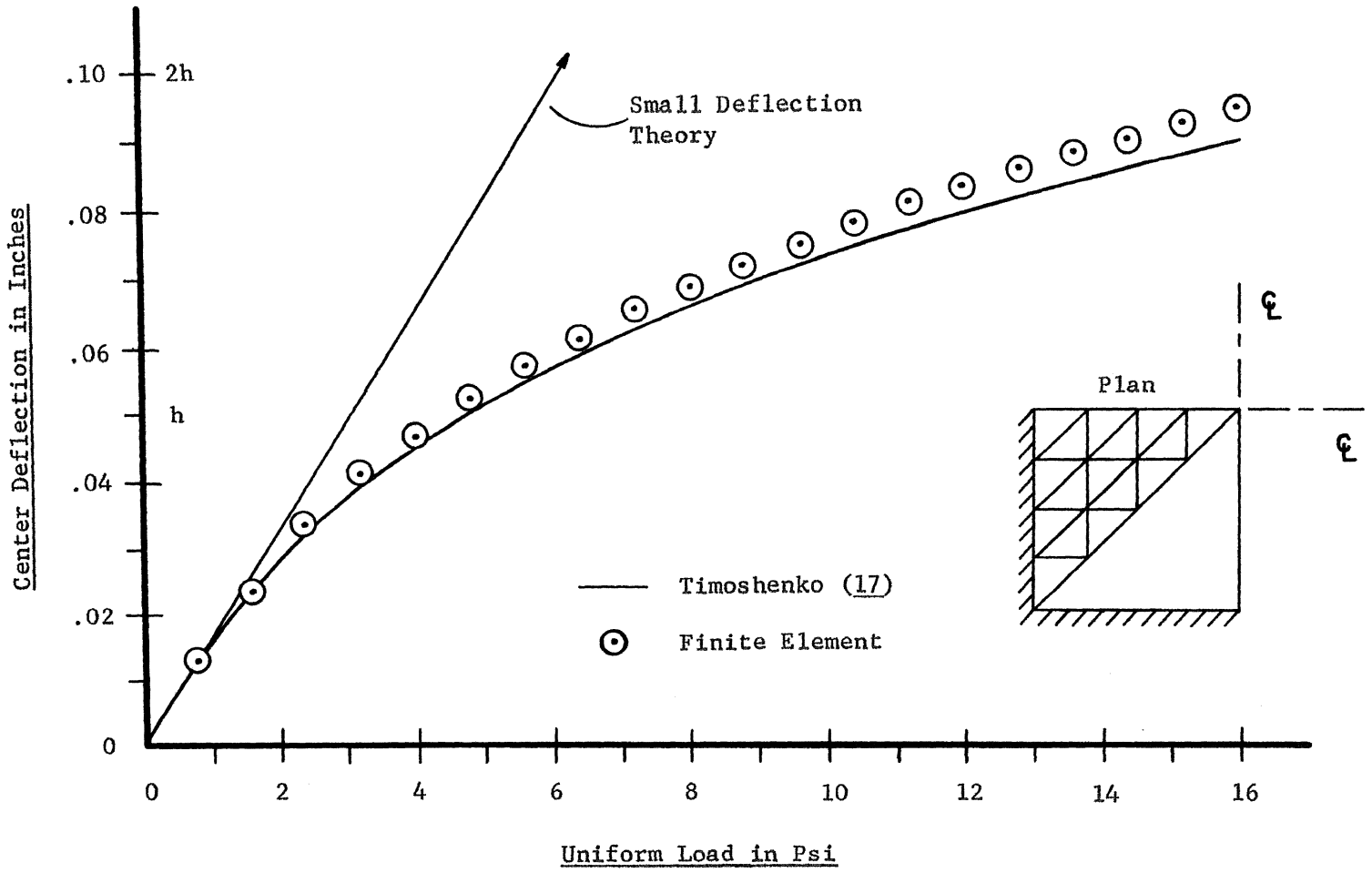

Figure 15. Load-Deflection of Rigidly Clamped Square Plate.

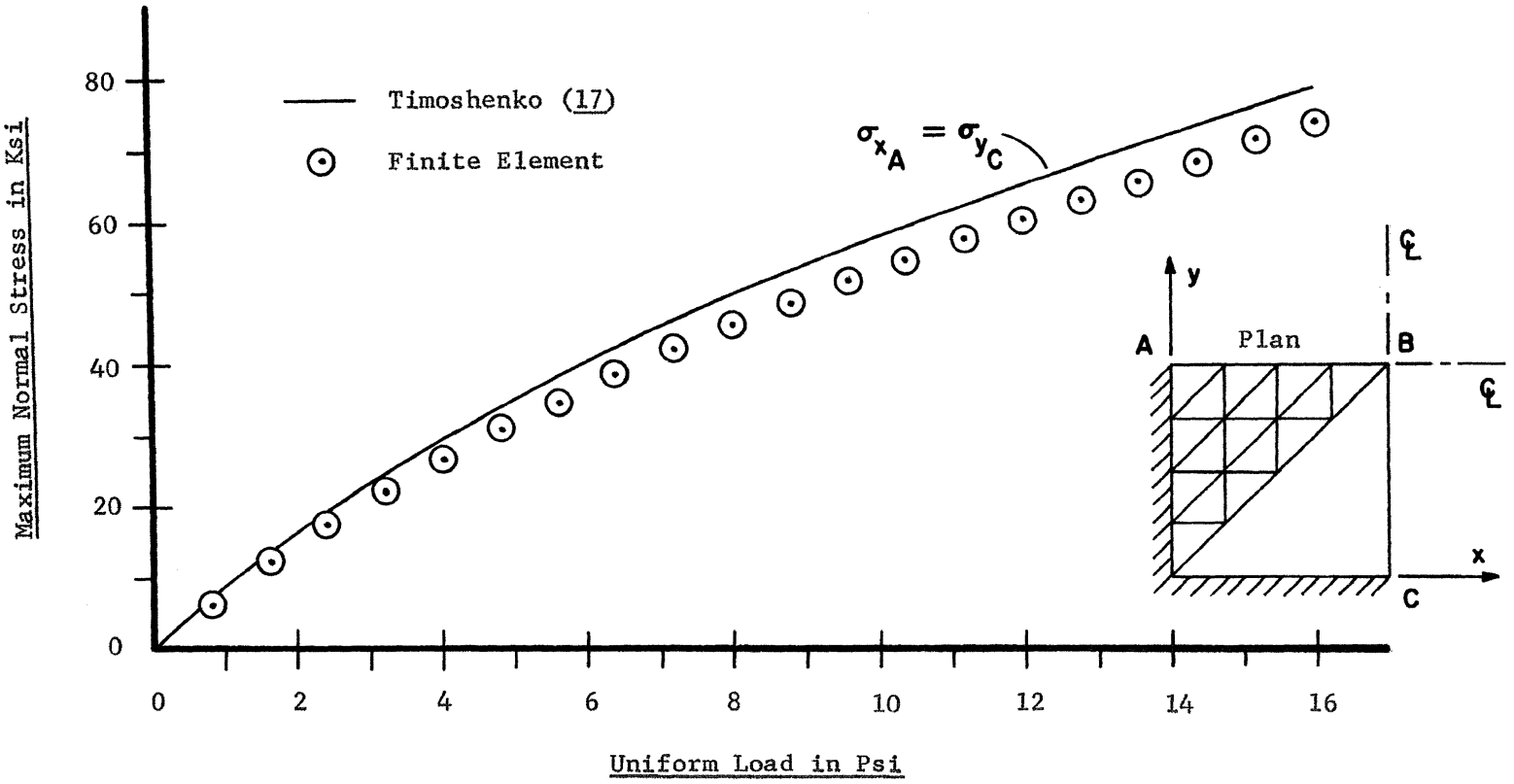

Figure 16. Maximum Stress in Rigidly Clamped Square Plate.

psi and a Poisson's ratio of 0.3 were used. A nonuniform mesh (see Figure 17) was employed utilizing a finer grid near the applied load and along edge A-B. The loading was applied in 10 equal steps with 3 iterations per step.

The deflections of a cantilevered plate of Berylco 25 beryllium-copper alloy, having the above dimensions and properties and subject to concentrated corner loads of 0.772 pounds and 1.544 pounds, were measured experimentally by Lin, et al. (19). A comparison between the experimental deflections of edge A-B and those from the finite element solution is given in Figure 17. Note the excellent agreement with the experimental values. This is encouraging in light of the fact that the maximum tip deflection was on the order of 100 times the plate thickness. Also, the maximum tip rotation was approximately 25 degrees. The finite element solution for the load of 1.544 pounds also yielded the solution for half the loading (0.772 pounds) and for each of the other loading levels as well. This applicability to progressive load increases is one of the assets of the incremental approach.

E. DISCUSSION OF RESULTS

The preceeding examples include problems involving various types of boundary conditions, the presence of large in-plane forces (examples A, B, and C), and large geometric displacements and rotations (example D). The results indicate that the macroscopic structural behavior is generally well represented by the model. The validity of the procedure for bending in two directions, as might occur in an arbitrary shell, has been demonstrated. It should be emphasized that although the technique and formulation have been used for specific large deflection

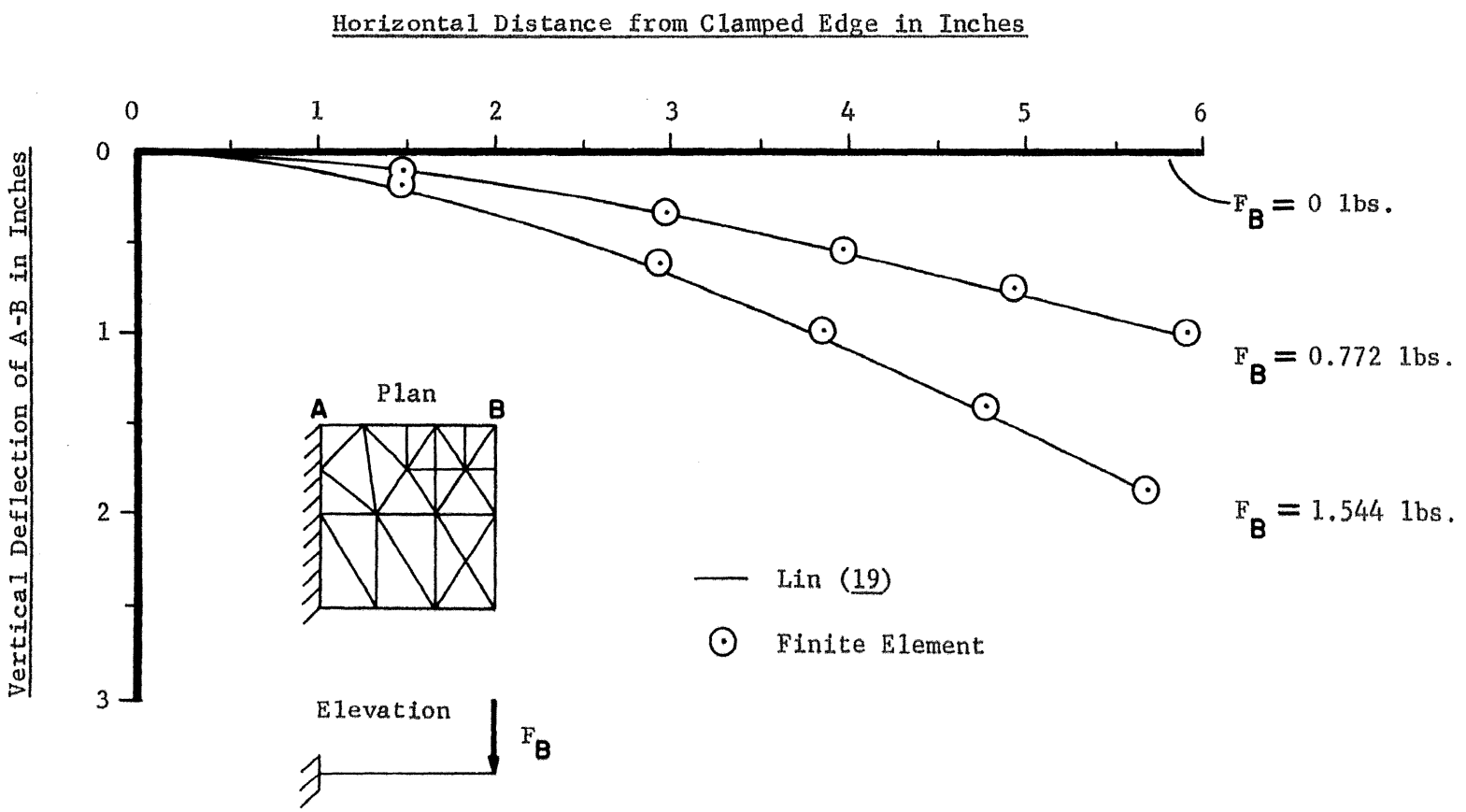

Figure 17. Deflection Curve for Leading Edge of Cantilevered Plate Subject to Different Corner Loads.

problems for plates of common shapes, the method can be applied to plates and shells of arbitrary geometry and boundary conditions for which no classical solution exists.

The extremely nonlinear cantilevered plate problem (example D), far beyond the scope of exact analytical solution, demonstrates the applicability of the proposed finite element method to geometrically nonlinear problems in shells. All the examples presented are essentially shell problems since appreciable deflection of a plate yields a doubly curved shell surface with bending in two directions.

The noticeable stiffening of the plates with increased loading in examples A, B, and C is due primarily to the induced membrane forces which resist further deflection. The 'geometrical' stiffness has been formulated to account for such an effect.

It was noted in the examples that agreement with the stress solutions of Levy and Timoshenko was not as good as for deflections. An accurate determination of stresses from a displacement model is always more difficult to achieve than a determination of displacements. The displacement model employed maintains normal slope compatibility along the element interfaces in the limit as the mesh size is reduced, but curvatures and hence stresses are discontinuous. The averaging of the stresses at the nodes, discussed in Chapter IV, hopefully minimizes this. Also, a discrepancy in stress results might be expected because the published results of Levy and Timoshenko employ a Lagrangian description. The finite element results are the true stresses. This is so because the stress increments for each step of the finite element method are based on the existing geometry at the beginning of that step.

The results of this chapter indicate that the proposed finite element method seems to be well adapted to obtaining solutions to nonlinear large deflection problems in thin plates and shells, which are sufficiently accurate for engineering purposes.

CHAPTER VII

CONCLUSIONS

A finite element method has been presented for obtaining numerical solutions to geometrically nonlinear large displacement problems in thin, elastic plates and shells. It has been demonstrated that this method is capable of solving a number of problems in which in-plane and out-of-plane behavior are coupled and that the results for displacements are sufficiently accurate for engineering purposes. The procedure has been shown to be sensitive to the step size and grid mesh employed.

The stress results did not compare as well with published results as did the displacements. A finer grid size along the boundaries and careful interpretation of results might yield a favorable comparison to experimentally measured stresses when they become available.

Further extensions of the proposed method to improve the results and to treat other classes of problems would be of considerable interest. These extensions can be itemized as follows:

(i) Optimization of numerical computations.

(ii) Refinement of the displacement model to ensure complete displacement compatibility.

(iii) Derivation of a symmetric 'geometrical' stiffness matrix from the energy approach.

(iv) Extension of the method to include nonlinear material properties as well as temperature effects.

(v) Utilization of the 'geometrical' stiffness concept to treat the eigenvalue problem in buckling instability.

BIBLIOGRAPHY

1. Turner, M. J., Dill, E. H., Martin, H. C., and Melosh, R. J., "Large Deflections of Structures Subjected to Heating and External Loads," J. of the Aerospace Sciences, 27, Feb. 1960, pp. 97-106.

2. Martin, H. C., "On the Derivation of Stiffness Matrices for the Analysis of Large Deflection and Stability Problems," Proceedings of the Conference on Matrix Methods in Structural Mechanics, TR-66-80, 1966, Wright-Patterson AFB, Ohio.

3. Argyris, J. H., "Matrix Analysis of Three-Dimensional Elastic Media, Small and Large Displacements," AIAA Journal, Vol. 3, No. 1, Jan. 1965, pp. 45-51.

4. Argyris, J. H., "Recent Advances in Matrix Methods of Structural Analysis," Progress in Aeronautical Sciences, Pergamon Press, London, New York, Vol. 4, 1963, pp. 115-145.

5. Argyris, J. H., "Continua and Discontinua," Proceedings of the Conference on Matrix Methods in Structural Mechanics, TR-66-80, 1966, Wright-Patterson AFB, Ohio.

6. Murray, D. W. and Wilson, E. L., "Finite-Element Large Deflection Analysis of Plates," J. of the Engr. Mech. Div., Proceedings of the A. S. C. E., Vol. 95, No. EM1, Feb. 1969, pp. 143-165.

7. Tezcan, S. S., "Nonlinear Analysis of Thin Plates by Framework Method," AIAA Journal, Vol. 5, No. 10, Oct. 1967, pp. 1890-1892.

8. Stricklin, J. A., Haisler, W. E., Mac Dougall, H. R. and Stebbins, F. J., "Nonlinear Analysis of Shells of Revolution by the Matrix Displacement Method," AIAA Journal, Vol. 6, No. 12, Dec. 1968, pp. 2306-2312.

9. Oden, J. T., "Numerical Formulation of Nonlinear Elasticity Problems," J. of the Struct. Div., Proceedings of the A. S. C. E., Vol. 93, No. ST3, June 1967, pp. 235-255.

10. Alzheimer, W. E. and Davis, R. T., "Nonlinear Unsymmetrical Bending of an Annular Plate," J. of Appl. Mech., Trans. of the A. S. M. E., March 1968, pp. 190-192.

11. Mallett, R. H. and Schmit, L. A., "Nonlinear Structural Analysis by Energy Search," J. of the Struct. Div., Proceedings of the A. S. C. E., Vol. 93, No. ST3, June 1967, pp. 221-234.

12. Schmit, L. A., Bogner, F. K. and Fox, R. L., "Finite Deflection Structural Analysis Using Plate and Shell Discrete Elements," AIAA Journal, Vol. 6, No. 5, May 1968, pp. 781-791.

13. Akyuz, F. A. and Merwin, J. E., "Solution of Nonlinear Problems of Elastoplasticity by the Finite Element Method," AIAA Journal, Vol. 6, No. 10, Oct. 1968, pp. 1825-1831.

14. Marcal, P. V., "Large Deflection Analysis of Elastic-Plastic Shells of Revolution," Proceedings of the AIAA/ASME 10th Structures, Structural Dynamics and Materials Conference, New Orleans, La., April 1969, pp. 369-379.

15. Zienkiewicz, O. C., The Finite Element Method in Structural and Continuum Mechanics, McGraw-Hill, New York, 1967.

16. Connor, J., "Bending of Thin Plates - Displacement Models," Special Summer Program 1.59S, June 1968, Massachusetts Institute of Technology, Cambridge, Massachusetts.

17. Timoshenko, S. and Woinowsky-Krieger, S., Theory of Plates and Shells, McGraw-Hill, New York, 2nd ed., 1959.

18. Levy, S., "Bending of Rectangular Plates with Large Deflections," NACA Technical Note 846, 1942.

19. Lin, T. H., Lin, S. R. and Mazelsky, B., "Large Inextensional Deflection of Thin Cantilevered Plates," J. of Appl. Mech., Trans. of the A. S. M. E., Dec. 1968, pp. 774-777.

APPENDIX I

MATRICES FOR BENDING FORMULATION

$$[C1] = \begin{bmatrix}
1 & -a_2 & 0 & 0 & a_2^2 & 0 & 0 & -a_2^3\, t^{(2)} & -a_2^3\, r^{(2)} \\
0 & 0 & 1 & 0 & 0 & -a_2 & 0 & 0 & 0 \\
0 & -1 & 0 & 0 & 2a_2 & 0 & 0 & -3a_2^2\, t^{(2)} & -3a_2^2\, r^{(2)} \\
1 & a_1 & 0 & a_1^2 & 0 & 0 & 0 & a_1^3\, t^{(1)} & a_1^3\, r^{(1)} \\
0 & 0 & 1 & 0 & 0 & a_1 & 0 & 0 & 0 \\
0 & -1 & 0 & -2a_1 & 0 & 0 & 0 & -3a_1^2\, t^{(1)} & -3a_1^2\, r^{(1)} \\
1 & 0 & c & 0 & 0 & 0 & c^2 & 0 & c^3 \\
0 & 0 & 1 & 0 & 0 & 0 & 2c & 0 & 3c^2 \\
0 & -1 & 0 & 0 & 0 & -c & 0 & -c^2 & 0
\end{bmatrix}$$

$$\left[\tilde{Q}\right]^{(1)} = \begin{bmatrix}
0 & 0 & 0 & -2 & 0 & 0 & 0 & -6x\, t^{(1)} & -6x\, r^{(1)} \\
0 & 0 & 0 & 0 & 0 & 0 & -2 & -2x & -6y \\
0 & 0 & 0 & 0 & 0 & -2 & 0 & -4y & 0
\end{bmatrix}$$

$$\left[\tilde{Q}\right]^{(2)} = \begin{bmatrix}
0 & 0 & 0 & 0 & -2 & 0 & 0 & -6x\, t^{(2)} & -6x\, r^{(2)} \\
0 & 0 & 0 & 0 & 0 & 0 & -2 & -2x & -6y \\
0 & 0 & 0 & 0 & 0 & -2 & 0 & -4y & 0
\end{bmatrix}$$

$B1^{(1)} = c\, a_1^2/6$, $B2^{(1)} = c^2\, a_1/6$, $B3^{(1)} = c^2\, a_1^2/24$

$B4^{(1)} = c\, a_1^3/12$, $B5^{(1)} = c^3\, a_1/12$, $A^{(1)} = c\, a_1/2$

$B1^{(2)} = -c\, a_2^2/6$, $B2^{(2)} = c^2\, a_2/6$, $B3^{(2)} = -c^2 a_2^2/24$

$B4^{(2)} = c\, a_2^3/12$, $B5^{(2)} = c^3\, a_2/12$, $A^{(2)} = c\, a_2/2$

$A12 = A^{(1)} + A^{(2)}$

$$\left[k^{b_1}\right]^{(1,2)} = \frac{E\,h^3}{12(1-\upsilon^2)} \begin{bmatrix} 0 & 0 & 0 & 0 & 0 & 0 & 0 & 0 & 0 \\ & 0 & 0 & 0 & 0 & 0 & 0 & 0 & 0 \\ & & 0 & 0 & 0 & 0 & 0 & 0 & 0 \\ & & & K44 & 0 & 0 & K47 & K48 & K49 \\ & & & & K55 & 0 & K57 & K58 & K59 \\ & & & & & K66 & 0 & K68 & 0 \\ & & SYMMETRIC & & & & K77 & K78 & K79 \\ & & & & & & & K88 & K89 \\ & & & & & & & & K99 \end{bmatrix}$$

where

$$K44 = 4A^{(1)}, \quad K47 = 4\nu A^{(1)}, \quad K48 = (12t^{(1)} + 4\nu)B1^{(1)}$$

$$K49 = 12r^{(1)}B1^{(1)} + 12\nu B2^{(1)}, \quad K55 = 4A^{(2)}, \quad K57 = 4\nu A^{(2)}$$

$$K58 = (12t^{(2)} + 4\nu)B1^{(2)}, \quad K59 = 12r^{(2)}B1^{(2)} + 12\nu B2^{(2)}$$

$$K66 = 2(1-\upsilon)A12, \quad K68 = 4(1-\upsilon)(B2^{(1)} + B2^{(2)}), \quad K77 = 4\,A12$$

$$K78 = (12t^{(1)}\upsilon + 4)B1^{(1)} + (12t^{(2)}\upsilon + 4)B1^{(2)}$$

$$K79 = 12r^{(1)}\upsilon\,B1^{(1)} + 12(B2^{(1)} + B2^{(2)}) + 12r^{(2)}\upsilon\,B1^{(2)}$$

$$K88 = (36(t^{(1)})^2 + 24\nu\,t^{(1)} + 4)B4^{(1)} + (36(t^{(2)})^2 + 24\nu\,t^{(2)} + 4)B4^{(2)} + 8(1-\nu)(B5^{(1)} + B5^{(2)})$$

$$K89 = (36r^{(1)}t^{(1)} + 12r^{(1)}\nu)B4^{(1)} + (36r^{(2)}t^{(2)} + 12r^{(2)}\nu)B4^{(2)} + (12 + 36t^{(1)}\nu)B3^{(1)} + (12 + 36t^{(2)}\nu)B3^{(2)}$$

$$K99 = 36(r^{(1)})^2B4^{(1)} + 36(r^{(2)})^2B4^{(2)} + 72\nu(r^{(1)}B3^{(1)} + r^{(2)}B3^{(2)}) + 36(B5^{(1)} + B5^{(2)})$$

APPENDIX II

MATRICES FOR IN - PLANE FORMULATION

$$\left[CP \right] = \frac{1}{c(a_1 + a_2)} \begin{bmatrix} ca_1 & 0 & ca_2 & 0 & 0 & 0 \\ -c & 0 & c & 0 & 0 & 0 \\ -a_1 & 0 & -a_2 & 0 & (a_1 + a_2) & 0 \\ 0 & ca_1 & 0 & ca_2 & 0 & 0 \\ 0 & -c & 0 & c & 0 & 0 \\ 0 & -a_1 & 0 & -a_2 & 0 & (a_1 + a_2) \end{bmatrix}$$

$$\left[B^P \right] = \frac{1}{c(a_1 + a_2)} \begin{bmatrix} -c & 0 & c & 0 & 0 & 0 \\ 0 & -a_1 & 0 & -a_2 & 0 & (a_1 + a_2) \\ -a_1 & -c & -a_2 & c & (a_1 + a_2) & 0 \end{bmatrix}$$

APPENDIX III

DERIVATION OF TRANSFORMATION MATRIX

The transformation matrix of direction cosines of angles formed between the local and global axes systems, $\left[\lambda\right]$, has components defined by

$$\left[\lambda\right] = \begin{bmatrix} \lambda_{x'x} & \lambda_{x'y} & \lambda_{x'z} \\ \lambda_{y'x} & \lambda_{y'y} & \lambda_{y'z} \\ \lambda_{z'x} & \lambda_{z'y} & \lambda_{z'z} \end{bmatrix} \tag{III-1}$$

in which $\lambda_{x'x}$ = cosine of the angle between the x' and x axes, etc. These axes systems and the characteristic dimensions of the triangular element in question are repeated in Figure 18 for convenience. The lengths of the sides i-j, j-k, and k-i, denoted respectively by l_{ij}, l_{jk}, and l_{ki}, can be defined in terms of nodal locations in global coordinates as

$$\begin{aligned} l_{ij} &= \left((x_j - x_i)^2 + (y_j - y_i)^2 + (z_j - z_i)^2 \right)^{\frac{1}{2}} \\ l_{jk} &= \left((x_k - x_j)^2 + (y_k - y_j)^2 + (z_k - z_j)^2 \right)^{\frac{1}{2}} \\ l_{ki} &= \left((x_i - x_k)^2 + (y_i - y_k)^2 + (z_i - z_k)^2 \right)^{\frac{1}{2}} \quad . \end{aligned} \tag{III-2}$$

By trigonometry it can be seen that

$$\begin{aligned} l_{ij} &= a_1 + a_2 \\ l_{ki}^2 &= c^2 + a_2^2 \\ l_{jk}^2 &= c^2 + a_1^2 \end{aligned} \tag{III-3}$$

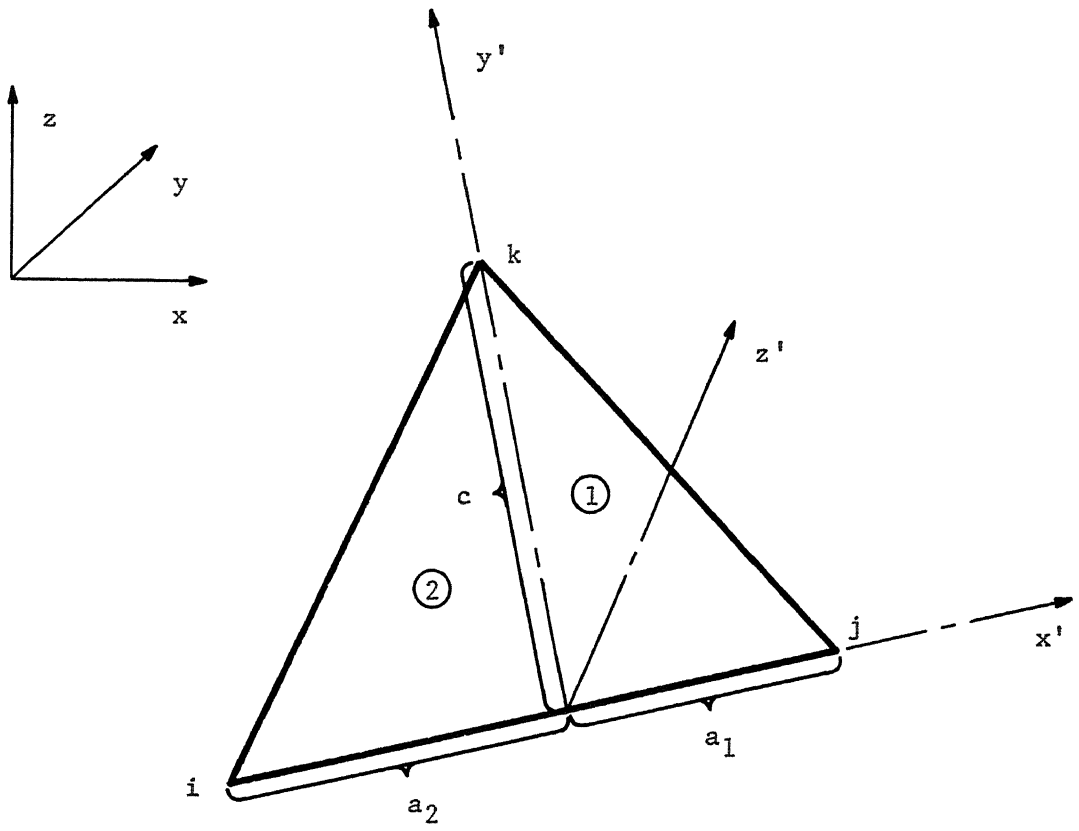

Figure 18. Triangular Element with Local and Global Coordinate Frames.

from which

$$a_2 = (l_{ij}^2 + l_{ki}^2 - l_{jk}^2)/2\, l_{ij}$$
$$a_1 = l_{ij} - a_2 \qquad \text{(III-4)}$$
$$c = (l_{ki}^2 - a_2^2)^{\frac{1}{2}} \quad .$$

The direction cosines of the x' axis are seen to be the same as for side i-j and are given by

$$\lambda_{x'x} = (x_j - x_i)/l_{ij}$$
$$\lambda_{x'y} = (y_j - y_i)/l_{ij} \qquad \text{(III-5)}$$
$$\lambda_{x'z} = (z_j - z_i)/l_{ij} \quad .$$

The components of a unit vector in the direction of the y' axis can be shown to be

$$\lambda_{y'x} = (x_k - x_i - a_2\, \lambda_{x'x})/c$$
$$\lambda_{y'y} = (y_k - y_i - a_2\, \lambda_{x'y})/c \qquad \text{(III-6)}$$
$$\lambda_{y'z} = (z_k - z_i - a_2\, \lambda_{x'z})/c$$

by subtracting the position vector of the origin of the primed system from the position vector of node k. For a right-handed local coordinate system, the unit vector in the z' direction is given in terms of unit vectors along the x' and y' axes by the cross product

$$\hat{e}_{z'} = \hat{e}_{x'} \times \hat{e}_{y'} \quad . \qquad \text{(III-7)}$$

The components of the unit vectors in the x' and y' directions, $\hat{e}_{x'}$ and $\hat{e}_{y'}$, respectively, are given in Equations (III-5) and (III-6). Performing the cross product gives the components of $\hat{e}_{z'}$ (the direction cosines of the z' axis) as

$$\begin{aligned} \lambda_{z'x} &= \lambda_{x'y}\ \lambda_{y'z} - \lambda_{x'z}\ \lambda_{y'y} \\ \lambda_{z'y} &= \lambda_{x'z}\ \lambda_{y'x} - \lambda_{x'x}\ \lambda_{y'z} \\ \lambda_{z'z} &= \lambda_{x'x}\ \lambda_{y'y} - \lambda_{x'y}\ \lambda_{y'x} \end{aligned} \qquad \text{(III-8)}$$

thus defining all the terms in Equation (III-1).

APPENDIX IV

GEOMETRICAL STIFFNESS SUBMATRICES

The $\left[6 \times 6\right]$ geometrical stiffness submatrices given in Chapter IV, section D by the matrix relation

$$\left[k_{rs_G}\right]^e = \left[L\right]^{T_e} \left[F_{rr}'\right]^e \left[\frac{\partial}{\partial \delta_s}\right] \tag{IV-1}$$

will be defined in the following.

In expanded form, Equation (IV-1) becomes

$$\left[k_{rs_G}\right]^e = \begin{bmatrix} RS(1,1) & RS(1,2) & RS(1,3) & 0 & 0 & 0 \\ RS(2,1) & RS(2,2) & RS(2,3) & 0 & 0 & 0 \\ RS(3,1) & RS(3,2) & RS(3,3) & 0 & 0 & 0 \\ RS(4,1) & RS(4,2) & RS(4,3) & 0 & 0 & 0 \\ RS(5,1) & RS(5,2) & RS(5,3) & 0 & 0 & 0 \\ RS(6,1) & RS(6,2) & RS(6,3) & 0 & 0 & 0 \end{bmatrix} \tag{IV-2}$$

where

$$RS(1,1) = F_{x_r}' \frac{\partial \lambda_{x'x}}{\partial x_s} + F_{y_r}' \frac{\partial \lambda_{y'x}}{\partial x_s} + F_{z_r}' \frac{\partial \lambda_{z'x}}{\partial x_s}$$

$$RS(1,2) = F_{x_r}' \frac{\partial \lambda_{x'x}}{\partial y_s} + F_{y_r}' \frac{\partial \lambda_{y'x}}{\partial y_s} + F_{z_r}' \frac{\partial \lambda_{z'x}}{\partial y_s}$$

$$RS(1,3) = F_{x_r}' \frac{\partial \lambda_{x'x}}{\partial z_s} + F_{y_r}' \frac{\partial \lambda_{y'x}}{\partial z_s} + F_{z_r}' \frac{\partial \lambda_{z'x}}{\partial z_s}$$

$$RS(2,1) = F_{x_r}' \frac{\partial \lambda_{x'y}}{\partial x_s} + F_{y_r}' \frac{\partial \lambda_{y'y}}{\partial x_s} + F_{z_r}' \frac{\partial \lambda_{z'y}}{\partial x_s}$$

$$RS(2,2) = F_{x_r}' \frac{\partial \lambda_{x'y}}{\partial y_s} + F_{y_r}' \frac{\partial \lambda_{y'y}}{\partial y_s} + F_{z_r}' \frac{\partial \lambda_{z'y}}{\partial y_s}$$

$$RS(2,3) = F_{x_r}' \frac{\partial \lambda_{x'y}}{\partial z_s} + F_{y_r}' \frac{\partial \lambda_{y'y}}{\partial z_s} + F_{z_r}' \frac{\partial \lambda_{z'y}}{\partial z_s}$$

$$RS(3,1) = F_{x_r}' \frac{\partial \lambda_{x'z}}{\partial x_s} + F_{y_r}' \frac{\partial \lambda_{y'z}}{\partial x_s} + F_{z_r}' \frac{\partial \lambda_{z'z}}{\partial x_s}$$

$$RS(3,2) = F_{x_r}' \frac{\partial \lambda_{x'z}}{\partial y_s} + F_{y_r}' \frac{\partial \lambda_{y'z}}{\partial y_s} + F_{z_r}' \frac{\partial \lambda_{z'z}}{\partial y_s}$$

$$RS(3,3) = F_{x_r}' \frac{\partial \lambda_{x'z}}{\partial z_s} + F_{yr}' \frac{\partial \lambda_{y'z}}{\partial z_s} + F_{z_r}' \frac{\partial \lambda_{z'z}}{\partial z_s}$$

$$RS(4,1) = M_{x_r}' \frac{\partial \lambda_{x'x}}{\partial x_s} + M_{y_r}' \frac{\partial \lambda_{y'x}}{\partial x_s} + M_{z_r}' \frac{\partial \lambda_{z'x}}{\partial x_s}$$

$$RS(4,2) = M_{x_r}' \frac{\partial \lambda_{x'x}}{\partial y_s} + M_{y_r}' \frac{\partial \lambda_{y'x}}{\partial y_s} + M_{z_r}' \frac{\partial \lambda_{z'x}}{\partial y_s}$$

$$RS(4,3) = M_{x_r}' \frac{\partial \lambda_{x'x}}{\partial z_s} + M_{y_r}' \frac{\partial \lambda_{y'x}}{\partial z_s} + M_{z_r}' \frac{\partial \lambda_{z'x}}{\partial z_s}$$

$$RS(5,1) = M_{x_r}' \frac{\partial \lambda_{x'y}}{\partial x_s} + M_{y_r}' \frac{\partial \lambda_{y'y}}{\partial x_s} + M_{z_r}' \frac{\partial \lambda_{z'y}}{\partial x_s}$$

$$RS(5,2) = M_{x_r}' \frac{\partial \lambda_{x'y}}{\partial y_s} + M_{y_r}' \frac{\partial \lambda_{y'y}}{\partial y_s} + M_{z_r}' \frac{\partial \lambda_{z'y}}{\partial y_s}$$

$$RS(5,3) = M_{x_r}' \frac{\partial \lambda_{x'y}}{\partial z_s} + M_{y_r}' \frac{\partial \lambda_{y'y}}{\partial z_s} + M_{z_r}' \frac{\partial \lambda_{z'y}}{\partial z_s}$$

$$RS(6,1) = M_{x_r}' \frac{\partial \lambda_{x'z}}{\partial x_s} + M_{y_r}' \frac{\partial \lambda_{y'z}}{\partial x_s} + M_{z_r}' \frac{\partial \lambda_{z'z}}{\partial x_s}$$

$$RS(6,2) = M_{x_r}' \frac{\partial \lambda_{x'z}}{\partial y_s} + M_{y_r}' \frac{\partial \lambda_{y'z}}{\partial y_s} + M_{z_r}' \frac{\partial \lambda_{z'z}}{\partial y_s}$$

$$RS(6,3) = M_{x_r}' \frac{\partial \lambda_{x'z}}{\partial z_s} + M_{y_r}' \frac{\partial \lambda_{y'z}}{\partial z_s} + M_{z_r}' \frac{\partial \lambda_{z'z}}{\partial z_s}$$

In the above equations, it is understood that r,s = i, j, k where i, j, and k are the nodes of the element in question. The partial derivatives

of the direction cosines appearing in these equations will be presented next for all values of s (i.e. s = i, j, k). For a definition of the direction cosines refer to Appendix III.

The following term groupings will be helpful in defining the partial derivatives:

$$A2XI = \frac{\partial a_2}{\partial x_i} = -\lambda_{x'x} + (x_i - x_k + a_2 \lambda_{x'x})/l_{ij}$$

$$A2XJ = \frac{\partial a_2}{\partial x_j} = (x_k - x_i - a_2 \lambda_{x'x})/l_{ij}$$

$$A2XK = \frac{\partial a_2}{\partial x_k} = \lambda_{x'x}$$

$$A2YI = \frac{\partial a_2}{\partial y_i} = -\lambda_{x'y} + (y_i - y_k + a_2 \lambda_{x'y})/l_{ij}$$

$$A2YJ = \frac{\partial a_2}{\partial y_j} = (y_k - y_i - a_2 \lambda_{x'y})/l_{ij}$$

$$A2YK = \frac{\partial a_2}{\partial y_k} = \lambda_{x'y}$$

$$A2ZI = \frac{\partial a_2}{\partial z_i} = -\lambda_{x'z} + (z_i - z_k + a_2 \lambda_{x'z})/l_{ij}$$

$$A2ZJ = \frac{\partial a_2}{\partial z_j} = (z_k - z_i - a_2 \lambda_{x'z})/l_{ij}$$

$$A2ZK = \frac{\partial a_2}{\partial z_k} = \lambda_{x'z}$$

$$CXI = \frac{\partial (1/c)}{\partial x_i} = (x_k - x_i + a_2\, A2XI)/c^3$$

$$CXJ = \frac{\partial (1/c)}{\partial x_j} = a_2\, A2XJ/c^3$$

$$CXK = \frac{\partial (1/c)}{\partial x_k} = (x_i - x_k + a_2\, A2XK)/c^3$$

$$CYI = \frac{\partial(1/c)}{\partial y_i} = (y_k - y_i + a_2 \; A2YI)/c^3$$

$$CYJ = \frac{\partial(1/c)}{\partial y_j} = a_2 \; A2YJ/c^3$$

$$CYK = \frac{\partial(1/c)}{\partial y_k} = (y_i - y_k + a_2 \; A2YK)/c^3$$

$$CZI = \frac{\partial(1/c)}{\partial z_i} = (z_k - z_i + a_2 \; A2ZI)/c^3$$

$$CZJ = \frac{\partial(1/c)}{\partial z_j} = a_2 \; A2ZJ/c^3$$

$$CZK = \frac{\partial(1/c)}{\partial z_k} = (z_i - z_k + a_2 \; A2ZK)/c^3$$

The partial derivatives of the direction cosines, with respect to the global nodal coordinates of the element in question, can now be defined as follows:

$$\frac{\partial \lambda_{x'x}}{\partial x_i} = -(1 - \lambda_{x'x}{}^2)/l_{ij}$$

$$\frac{\partial \lambda_{x'x}}{\partial x_j} = (1 - \lambda_{x'x}{}^2)/l_{ij}$$

$$\frac{\partial \lambda_{x'x}}{\partial x_k} = 0$$

$$\frac{\partial \lambda_{x'x}}{\partial y_i} = \lambda_{x'x} \; \lambda_{x'y}/l_{ij}$$

$$\frac{\partial \lambda_{x'x}}{\partial y_j} = -\lambda_{x'x} \; \lambda_{x'y}/l_{ij}$$

$$\frac{\partial \lambda_{x'x}}{\partial y_k} = 0$$

$$\frac{\partial \lambda_{x'x}}{\partial z_i} = \lambda_{x'x}\ \lambda_{x'z}/l_{ij}$$

$$\frac{\partial \lambda_{x'x}}{\partial z_j} = -\ \lambda_{x'x}\ \lambda_{x'z}/l_{ij}$$

$$\frac{\partial \lambda_{x'x}}{\partial z_k} = 0$$

$$\frac{\partial \lambda_{x'y}}{\partial x_i} = \lambda_{x'x}\ \lambda_{x'y}/l_{ij}$$

$$\frac{\partial \lambda_{x'y}}{\partial x_j} = -\ \lambda_{x'x}\ \lambda_{x'y}/l_{ij}$$

$$\frac{\partial \lambda_{x'y}}{\partial x_k} = 0$$

$$\frac{\partial \lambda_{x'y}}{\partial y_i} = -\ (1 - \lambda_{x'y}^2)/l_{ij}$$

$$\frac{\partial \lambda_{x'y}}{\partial y_j} = (1 - \lambda_{x'y}^2)/l_{ij}$$

$$\frac{\partial \lambda_{x'y}}{\partial y_k} = 0$$

$$\frac{\partial \lambda_{x'y}}{\partial z_i} = \lambda_{x'y}\ \lambda_{x'z}/l_{ij}$$

$$\frac{\partial \lambda_{x'y}}{\partial z_j} = -\ \lambda_{x'y}\ \lambda_{x'z}/l_{ij}$$

$$\frac{\partial \lambda_{x'y}}{\partial z_k} = 0$$

$$\frac{\partial \lambda_{x'z}}{\partial x_i} = \lambda_{x'x}\ \lambda_{x'z}/l_{ij}$$

$$\frac{\partial \lambda_{x'z}}{\partial x_j} = -\ \lambda_{x'x}\ \lambda_{x'z}/l_{ij}$$

$$\frac{\partial \lambda_{x'z}}{\partial x_k} = 0$$

$$\frac{\partial \lambda_{x'z}}{\partial y_i} = \lambda_{x'y}\ \lambda_{x'z}/l_{ij}$$

$$\frac{\partial \lambda_{x'z}}{\partial y_j} = -\ \lambda_{x'y}\ \lambda_{x'z}/l_{ij}$$

$$\frac{\partial \lambda_{x'z}}{\partial y_k} = 0$$

$$\frac{\partial \lambda_{x'z}}{\partial z_i} = -\ (1-\ \lambda_{x'z}{}^2)/l_{ij}$$

$$\frac{\partial \lambda_{x'z}}{\partial z_j} = (1-\ \lambda_{x'z}{}^2)/l_{ij}$$

$$\frac{\partial \lambda_{x'z}}{\partial z_k} = 0$$

$$\frac{\partial \lambda_{y'x}}{\partial x_i} = -\ 1/c\ +\ (x_k - x_i)\ CXI - \lambda_{x'x}\ A2XI/c - a_2\ \lambda_{x'x}\ CXI - a_2\ \frac{\partial \lambda_{x'x}}{\partial x_i} \Big/ c$$

$$\frac{\partial \lambda_{y'x}}{\partial x_j} = (x_k - x_i)\ CXJ - \lambda_{x'x}\ A2XJ/c - a_2\ \lambda_{x'x}\ CXJ - a_2\ \frac{\partial \lambda_{x'x}}{\partial x_j} \Big/ c$$

$$\frac{\partial \lambda_{y'x}}{\partial x_k} = 1/c + (x_k - x_i)\,CXK - \lambda_{x'x}\,A2XK/c - a_2\,\lambda_{x'x}\,CXK - a_2\,\frac{\partial \lambda_{x'x}}{\partial x_k} \Big/ c$$

$$\frac{\partial \lambda_{y'x}}{\partial y_i} = (x_k - x_i)\,CYI - \lambda_{x'x}\,A2YI/c - a_2\,\lambda_{x'x}\,CYI - a_2\,\frac{\partial \lambda_{x'x}}{\partial y_i} \Big/ c$$

$$\frac{\partial \lambda_{y'x}}{\partial y_j} = (x_k - x_i)\,CYJ - \lambda_{x'x}\,A2YJ/c - a_2\,\lambda_{x'x}\,CYJ - a_2\,\frac{\partial \lambda_{x'x}}{\partial y_j} \Big/ c$$

$$\frac{\partial \lambda_{y'x}}{\partial y_k} = (x_k - x_i)\,CYK - \lambda_{x'x}\,A2YK/c - a_2\,\lambda_{x'x}\,CYK - a_2\,\frac{\partial \lambda_{x'x}}{\partial y_k} \Big/ c$$

$$\frac{\partial \lambda_{y'x}}{\partial z_i} = (x_k - x_i)\,CZI - \lambda_{x'x}\,A2ZI/c - a_2\,\lambda_{x'x}\,CZI - a_2\,\frac{\partial \lambda_{x'x}}{\partial z_i} \Big/ c$$

$$\frac{\partial \lambda_{y'x}}{\partial z_j} = (x_k - x_i)\,CZJ - \lambda_{x'x}\,A2ZJ/c - a_2\,\lambda_{x'x}\,CZJ - a_2\,\frac{\partial \lambda_{x'x}}{\partial z_j} \Big/ c$$

$$\frac{\partial \lambda_{y'x}}{\partial z_k} = (x_k - x_i)\,CZK - \lambda_{x'x}\,A2ZK/c - a_2\,\lambda_{x'x}\,CZK - a_2\,\frac{\partial \lambda_{x'x}}{\partial z_k} \Big/ c$$

$$\frac{\partial \lambda_{y'y}}{\partial x_i} = (y_k - y_i)\ CXI - \lambda_{x'y}\ A2XI/c - a_2\ \lambda_{x'y}\ CXI - a_2 \frac{\partial \lambda_{x'y}}{\partial x_i} \Big/ c$$

$$\frac{\partial \lambda_{y'y}}{\partial x_j} = (y_k - y_i)\ CXJ - \lambda_{x'y}\ A2XJ/c - a_2\ \lambda_{x'y}\ CXJ - a_2 \frac{\partial \lambda_{x'y}}{\partial x_j} \Big/ c$$

$$\frac{\partial \lambda_{y'y}}{\partial x_k} = (y_k - y_i)\ CXK - \lambda_{x'y}\ A2XK/c - a_2\ \lambda_{x'y}\ CXK - a_2 \frac{\partial \lambda_{x'y}}{\partial x_k} \Big/ c$$

$$\frac{\partial \lambda_{y'y}}{\partial y_i} = -1/c + (y_k - y_i)\ CYI - \lambda_{x'y}\ A2YI/c - a_2\ \lambda_{x'y}\ CYI - a_2 \frac{\partial \lambda_{x'y}}{\partial y_i} \Big/ c$$

$$\frac{\partial \lambda_{y'y}}{\partial y_j} = (y_k - y_i)\ CYJ - \lambda_{x'y}\ A2YJ/c - a_2\ \lambda_{x'y}\ CYJ - a_2 \frac{\partial \lambda_{x'y}}{\partial y_j} \Big/ c$$

$$\frac{\partial \lambda_{y'y}}{\partial y_k} = 1/c + (y_k - y_i)\ CYK - \lambda_{x'y}\ A2YK/c - a_2\ \lambda_{x'y}\ CYK - a_2 \frac{\partial \lambda_{x'y}}{\partial y_k} \Big/ c$$

$$\frac{\partial \lambda_{y'y}}{\partial z_i} = (y_k - y_i)\ CZI - \lambda_{x'y}\ A2ZI/c - a_2\ \lambda_{x'y}\ CZI - a_2 \frac{\partial \lambda_{x'y}}{\partial z_i} \Big/ c$$

$$\frac{\partial \lambda_{y'y}}{\partial z_j} = (y_k - y_i)\ CZJ - \lambda_{x'y}\ A2ZJ/c - a_2\ \lambda_{x'y}\ CZJ - a_2 \frac{\partial \lambda_{x'y}}{\partial z_j} \Big/ c$$

$$\frac{\partial \lambda_{y'y}}{\partial z_k} = (y_k - y_i)\ CZK - \lambda_{x'y}\ A2ZK/c - a_2\ \lambda_{x'y}\ CZK - a_2 \frac{\partial \lambda_{x'y}}{\partial z_k} \Big/ c$$

$$\frac{\partial \lambda_{y'z}}{\partial x_i} = (z_k - z_i)\ CXI - \lambda_{x'z}\ A2XI/c - a_2\ \lambda_{x'z}\ CXI - a_2 \frac{\partial \lambda_{x'z}}{\partial x_i} \Big/ c$$

$$\frac{\partial \lambda_{y'z}}{\partial x_j} = (z_k - z_i)\ CXJ - \lambda_{x'z}\ A2XJ/c - a_2\ \lambda_{x'z}\ CXJ - a_2 \frac{\partial \lambda_{x'z}}{\partial x_j} \Big/ c$$

$$\frac{\partial \lambda_{y'z}}{\partial x_k} = (z_k - z_i)\ CXK - \lambda_{x'z}\ A2XK/c - a_2\ \lambda_{x'z}\ CXK - a_2 \frac{\partial \lambda_{x'z}}{\partial x_k} \Big/ c$$

$$\frac{\partial \lambda_{y'z}}{\partial y_i} = (z_k - z_i)\ CYI - \lambda_{x'z}\ A2YI/c - a_2\ \lambda_{x'z}\ CYI - a_2 \frac{\partial \lambda_{x'z}}{\partial y_i} \Big/ c$$

$$\frac{\partial \lambda_{y'z}}{\partial y_j} = (z_k - z_i)\ CYJ - \lambda_{x'z}\ A2YJ/c - a_2\ \lambda_{x'z}\ CYJ - a_2 \frac{\partial \lambda_{x'z}}{\partial y_j} \Big/ c$$

$$\frac{\partial \lambda_{y'z}}{\partial y_k} = (z_k - z_i)\ CYK - \lambda_{x'z}\ A2YK/c - a_2\ \lambda_{x'z}\ CYK - a_2 \frac{\partial \lambda_{x'z}}{\partial y_k} \Big/ c$$

$$\frac{\partial \lambda_{y'z}}{\partial z_i} = -1/c + (z_k - z_i)\ CZI - \lambda_{x'z}\ A2ZI/c - a_2\ \lambda_{x'z}\ CZI - a_2 \frac{\partial \lambda_{x'z}}{\partial z_i} \Big/ c$$

$$\frac{\partial \lambda_{y'z}}{\partial z_j} = (z_k - z_i)\ CZJ - \lambda_{x'z}\ A2ZJ/c - a_2\ \lambda_{x'z}\ CZJ - a_2 \frac{\partial \lambda_{x'z}}{\partial z_j} \Big/ c$$

$$\frac{\partial \lambda_{y'z}}{\partial z_k} = 1/c + (z_k - z_i)\ CZK - \lambda_{x'z}\ A2ZK/c - a_2\ \lambda_{x'z}\ CZK - a_2 \frac{\partial \lambda_{x'z}}{\partial z_k} \Big/ c$$

$$\frac{\partial \lambda_{z'x}}{\partial x_i} = \lambda_{x'y} \frac{\partial \lambda_{y'z}}{\partial x_i} + \lambda_{y'z} \frac{\partial \lambda_{x'y}}{\partial x_i} - \lambda_{x'z} \frac{\partial \lambda_{y'y}}{\partial x_i} - \lambda_{y'y} \frac{\partial \lambda_{x'z}}{\partial x_i}$$

$$\frac{\partial \lambda_{z'x}}{\partial x_j} = \lambda_{x'y} \frac{\partial \lambda_{y'z}}{\partial x_j} + \lambda_{y'z} \frac{\partial \lambda_{x'y}}{\partial x_j} - \lambda_{x'z} \frac{\partial \lambda_{y'y}}{\partial x_j} - \lambda_{y'y} \frac{\partial \lambda_{x'z}}{\partial x_j}$$

$$\frac{\partial \lambda_{z'x}}{\partial x_k} = \lambda_{x'y} \frac{\partial \lambda_{y'z}}{\partial x_k} + \lambda_{y'z} \frac{\partial \lambda_{x'y}}{\partial x_k} - \lambda_{x'z} \frac{\partial \lambda_{y'y}}{\partial x_k} - \lambda_{y'y} \frac{\partial \lambda_{x'z}}{\partial x_k}$$

$$\frac{\partial \lambda_{z'x}}{\partial y_i} = \lambda_{x'y} \frac{\partial \lambda_{y'z}}{\partial y_i} + \lambda_{y'z} \frac{\partial \lambda_{x'y}}{\partial y_i} - \lambda_{x'z} \frac{\partial \lambda_{y'y}}{\partial y_i} - \lambda_{y'y} \frac{\partial \lambda_{x'z}}{\partial y_i}$$

$$\frac{\partial \lambda_{z'x}}{\partial y_j} = \lambda_{x'y}\frac{\partial \lambda_{y'z}}{\partial y_j} + \lambda_{y'z}\frac{\partial \lambda_{x'y}}{\partial y_j} - \lambda_{x'z}\frac{\partial \lambda_{y'y}}{\partial y_j} - \lambda_{y'y}\frac{\partial \lambda_{x'z}}{\partial y_j}$$

$$\frac{\partial \lambda_{z'x}}{\partial y_k} = \lambda_{x'y}\frac{\partial \lambda_{y'z}}{\partial y_k} + \lambda_{y'z}\frac{\partial \lambda_{x'y}}{\partial y_k} - \lambda_{x'z}\frac{\partial \lambda_{y'y}}{\partial y_k} - \lambda_{y'y}\frac{\partial \lambda_{x'z}}{\partial y_k}$$

$$\frac{\partial \lambda_{z'x}}{\partial z_i} = \lambda_{x'y}\frac{\partial \lambda_{y'z}}{\partial z_i} + \lambda_{y'z}\frac{\partial \lambda_{x'y}}{\partial z_i} - \lambda_{x'z}\frac{\partial \lambda_{y'y}}{\partial z_i} - \lambda_{y'y}\frac{\partial \lambda_{x'z}}{\partial z_i}$$

$$\frac{\partial \lambda_{z'x}}{\partial z_j} = \lambda_{x'y}\frac{\partial \lambda_{y'z}}{\partial z_j} + \lambda_{y'z}\frac{\partial \lambda_{x'y}}{\partial z_j} - \lambda_{x'z}\frac{\partial \lambda_{y'y}}{\partial z_j} - \lambda_{y'y}\frac{\partial \lambda_{x'z}}{\partial z_j}$$

$$\frac{\partial \lambda_{z'x}}{\partial z_k} = \lambda_{x'y}\frac{\partial \lambda_{y'z}}{\partial z_k} + \lambda_{y'z}\frac{\partial \lambda_{x'y}}{\partial z_k} - \lambda_{x'z}\frac{\partial \lambda_{y'y}}{\partial z_k} - \lambda_{y'y}\frac{\partial \lambda_{x'z}}{\partial z_k}$$

$$\frac{\partial \lambda_{z'y}}{\partial x_i} = \lambda_{x'z}\frac{\partial \lambda_{y'x}}{\partial x_i} + \lambda_{y'x}\frac{\partial \lambda_{x'z}}{\partial x_i} - \lambda_{x'x}\frac{\partial \lambda_{y'z}}{\partial x_i} - \lambda_{y'z}\frac{\partial \lambda_{x'x}}{\partial x_i}$$

$$\frac{\partial \lambda_{z'y}}{\partial x_j} = \lambda_{x'z}\frac{\partial \lambda_{y'x}}{\partial x_j} + \lambda_{y'x}\frac{\partial \lambda_{x'z}}{\partial x_j} - \lambda_{x'x}\frac{\partial \lambda_{y'z}}{\partial x_j} - \lambda_{y'z}\frac{\partial \lambda_{x'x}}{\partial x_j}$$

$$\frac{\partial \lambda_{z'y}}{\partial x_k} = \lambda_{x'z}\frac{\partial \lambda_{y'x}}{\partial x_k} + \lambda_{y'x}\frac{\partial \lambda_{x'z}}{\partial x_k} - \lambda_{x'x}\frac{\partial \lambda_{y'z}}{\partial x_k} - \lambda_{y'z}\frac{\partial \lambda_{x'x}}{\partial x_k}$$

$$\frac{\partial \lambda_{z'y}}{\partial y_i} = \lambda_{x'z}\frac{\partial \lambda_{y'x}}{\partial y_i} + \lambda_{y'x}\frac{\partial \lambda_{x'z}}{\partial y_i} - \lambda_{x'x}\frac{\partial \lambda_{y'z}}{\partial y_i} - \lambda_{y'z}\frac{\partial \lambda_{x'x}}{\partial y_i}$$

$$\frac{\partial \lambda_{z'y}}{\partial y_j} = \lambda_{x'z}\frac{\partial \lambda_{y'x}}{\partial y_j} + \lambda_{y'x}\frac{\partial \lambda_{x'z}}{\partial y_j} - \lambda_{x'x}\frac{\partial \lambda_{y'z}}{\partial y_j} - \lambda_{y'z}\frac{\partial \lambda_{x'x}}{\partial y_j}$$

$$\frac{\partial \lambda_{z'y}}{\partial y_k} = \lambda_{x'z}\frac{\partial \lambda_{y'x}}{\partial y_k} + \lambda_{y'x}\frac{\partial \lambda_{x'z}}{\partial y_k} - \lambda_{x'x}\frac{\partial \lambda_{y'z}}{\partial y_k} - \lambda_{y'z}\frac{\partial \lambda_{x'x}}{\partial y_k}$$

$$\frac{\partial \lambda_{z'y}}{\partial z_i} = \lambda_{x'z}\frac{\partial \lambda_{y'x}}{\partial z_i} + \lambda_{y'x}\frac{\partial \lambda_{x'z}}{\partial z_i} - \lambda_{x'x}\frac{\partial \lambda_{y'z}}{\partial z_i} - \lambda_{y'z}\frac{\partial \lambda_{x'x}}{\partial z_i}$$

$$\frac{\partial \lambda_{z'y}}{\partial z_j} = \lambda_{x'z}\frac{\partial \lambda_{y'x}}{\partial z_j} + \lambda_{y'x}\frac{\partial \lambda_{x'z}}{\partial z_j} - \lambda_{x'x}\frac{\partial \lambda_{y'z}}{\partial z_j} - \lambda_{y'z}\frac{\partial \lambda_{x'x}}{\partial z_j}$$

$$\frac{\partial \lambda_{z'y}}{\partial z_k} = \lambda_{x'z}\frac{\partial \lambda_{y'x}}{\partial z_k} + \lambda_{y'x}\frac{\partial \lambda_{x'z}}{\partial z_k} - \lambda_{x'x}\frac{\partial \lambda_{y'z}}{\partial z_k} - \lambda_{y'z}\frac{\partial \lambda_{x'x}}{\partial z_k}$$

$$\frac{\partial \lambda_{z'z}}{\partial x_i} = \lambda_{x'x}\frac{\partial \lambda_{y'y}}{\partial x_i} + \lambda_{y'y}\frac{\partial \lambda_{x'x}}{\partial x_i} - \lambda_{x'y}\frac{\partial \lambda_{y'x}}{\partial x_i} - \lambda_{y'x}\frac{\partial \lambda_{x'y}}{\partial x_i}$$

$$\frac{\partial \lambda_{z'z}}{\partial x_j} = \lambda_{x'x}\frac{\partial \lambda_{y'y}}{\partial x_j} + \lambda_{y'y}\frac{\partial \lambda_{x'x}}{\partial x_j} - \lambda_{x'y}\frac{\partial \lambda_{y'x}}{\partial x_j} - \lambda_{y'x}\frac{\partial \lambda_{x'y}}{\partial x_j}$$

$$\frac{\partial \lambda_{z'z}}{\partial x_k} = \lambda_{x'x}\frac{\partial \lambda_{y'y}}{\partial x_k} + \lambda_{y'y}\frac{\partial \lambda_{x'x}}{\partial x_k} - \lambda_{x'y}\frac{\partial \lambda_{y'x}}{\partial x_k} - \lambda_{y'x}\frac{\partial \lambda_{x'y}}{\partial x_k}$$

$$\frac{\partial \lambda_{z'z}}{\partial y_i} = \lambda_{x'x}\frac{\partial \lambda_{y'y}}{\partial y_i} + \lambda_{y'y}\frac{\partial \lambda_{x'x}}{\partial y_i} - \lambda_{x'y}\frac{\partial \lambda_{y'x}}{\partial y_i} - \lambda_{y'x}\frac{\partial \lambda_{x'y}}{\partial y_i}$$

$$\frac{\partial \lambda_{z'z}}{\partial y_j} = \lambda_{x'x}\frac{\partial \lambda_{y'y}}{\partial y_j} + \lambda_{y'y}\frac{\partial \lambda_{x'x}}{\partial y_j} - \lambda_{x'y}\frac{\partial \lambda_{y'x}}{\partial y_j} - \lambda_{y'x}\frac{\partial \lambda_{x'y}}{\partial y_j}$$

$$\frac{\partial \lambda_{z'z}}{\partial y_k} = \lambda_{x'x}\frac{\partial \lambda_{y'y}}{\partial y_k} + \lambda_{y'y}\frac{\partial \lambda_{x'x}}{\partial y_k} - \lambda_{x'y}\frac{\partial \lambda_{y'x}}{\partial y_k} - \lambda_{y'x}\frac{\partial \lambda_{x'y}}{\partial y_k}$$

$$\frac{\partial \lambda_{z'z}}{\partial z_i} = \lambda_{x'x}\frac{\partial \lambda_{y'y}}{\partial z_i} + \lambda_{y'y}\frac{\partial \lambda_{x'x}}{\partial z_i} - \lambda_{x'y}\frac{\partial \lambda_{y'x}}{\partial z_i} - \lambda_{y'x}\frac{\partial \lambda_{x'y}}{\partial z_i}$$

$$\frac{\partial \lambda_{z'z}}{\partial z_j} = \lambda_{x'x}\frac{\partial \lambda_{y'y}}{\partial z_j} + \lambda_{y'y}\frac{\partial \lambda_{x'x}}{\partial z_j} - \lambda_{x'y}\frac{\partial \lambda_{y'x}}{\partial z_j} - \lambda_{y'x}\frac{\partial \lambda_{x'y}}{\partial z_j}$$

$$\frac{\partial \lambda_{z'z}}{\partial z_k} = \lambda_{x'x}\frac{\partial \lambda_{y'y}}{\partial z_k} + \lambda_{y'y}\frac{\partial \lambda_{x'x}}{\partial z_k} - \lambda_{x'y}\frac{\partial \lambda_{y'x}}{\partial z_k} - \lambda_{y'x}\frac{\partial \lambda_{x'y}}{\partial z_k} .$$

The preceeding relations completely define the geometrical stiffness submatrices $\left[k_{rs_G}\right]^e$ for element 'e' with nodes i, j, and k.

APPENDIX V

COMPUTER PROGRAM

The computer program written for this investigation was specialized to apply only to large displacement problems in initially flat plates. For specification of prescribed displacements, the global x-y plane was chosen as the mid-surface plane of the plate.

The program provides the option of specification of displacements along boundaries in the x-y plane that are oblique to the x and y directions. An iteration option can be utilized by supplying the number of iterates per incremental step as input data. Also, an option is available to allow the machine to calculate a 'consistent' load matrix corresponding to a uniform normal pressure on the entire plate. This eliminates the necessity of hand calculating and inputting the statically equivalent nodal loads corresponding to a uniform pressure.

Due to the length of the main line and the limited core storage available for the compiler, it was necessary to run the program under single partition. Computing time estimates for a specific problem can be obtained by referring to the discussion in Chapter V.

The input instructions and program listing could not be included. However, they are available from the author.

VITA

Ronald August Melliere, the son of Mr. and Mrs. Xavier Melliere, was born on August 12, 1944, in St. Louis, Missouri.

He received his primary education in Prairie du Rocher, Illinois, attended Red Bud High School in Red Bud, Illinois, and graduated in May, 1962. In September, 1962, he enrolled in Missouri School of Mines and Metallurgy and completed requirements for a Bachelor of Science degree in Mechanical Engineering in May, 1966.

In September, 1966, he enrolled in the Graduate School at the University of Missouri at Rolla, and completed the requirements for a Master of Science degree in Mechanical Engineering in August, 1967. He was admitted as a candidate for the degree of Doctor of Philosophy in Mechanical Engineering in September, 1967, and has since been so enrolled in the Graduate School at the University of Missouri at Rolla. He has held an NDEA Fellowship from September, 1966 to August, 1969.

He was married to Miss Jeanette Hahn on August 30, 1969.